

**THE INFLUENCE OF GRAPHENE ON THE MECHANICAL
PROPERTIES AND HYDROTHERMAL AGING OF 3 MOL%
YTTRIA STABILISED TETRAGONAL ZIRCONIA
POLYCRYSTALLINE AT VARIOUS SINTERING CONDITIONS**

CHONG CHEE HUNG


**A project report submitted in partial fulfilment of the
requirements for the award of Bachelor of Engineering
(Honours) Mechanical Engineering**

**Lee Kong Chian Faculty of Engineering and Science
Universiti Tunku Abdul Rahman**

May 2020

DECLARATION

I hereby declare that this project report is based on my original work except for citations and quotations which have been duly acknowledged. I also declare that it has not been previously and concurrently submitted for any other degree or award at UTAR or other institutions.

Signature :  _____

Name : Chong Chee Hung _____

ID No. : 1503881 _____

Date : 15 May 2020 _____

APPROVAL FOR SUBMISSION

I certify that this project report entitled “**THE INFLUENCE OF GRAPHENE ON THE MECHANICAL PROPERTIES AND HYDROTHERMAL AGING OF 3 MOL% YTTRIA STABILISED TETRAGONAL ZIRCONIA POLYCRYSTALLINE AT VARIOUS SINTERING CONDITIONS**” was prepared by **CHONG CHEE HUNG** has met the required standard for submission in partial fulfilment of the requirements for the award of Bachelor of Engineering (Hons.) Mechanical Engineering at Universiti Tunku Abdul Rahman.

Approved by,

Signature

:



Supervisor

:

Dr. Ting Chen Hunt

Date

:

15 May 2020

Signature

:

Co-Supervisor

:

Date

:

The copyright of this report belongs to the author under the terms of the copyright Act 1987 as qualified by Intellectual Property Policy of Universiti Tunku Abdul Rahman. Due acknowledgement shall always be made of the use of any material contained in, or derived from, this report.

© 2020, Chong Chee Hung. All right reserved.

ACKNOWLEDGEMENTS

First and foremost, I would like express my gratitude to Universiti Tunku Abdul Rahman (UTAR) for providing me an opportunity to conduct the research on my last year of study in degree. Through this opportunity, I am able to gain more insightful experiences to prepare myself for my future career path. Besides that, this research also enlightened my passion towards material engineering field.

I would also like to convey my appreciation to my supervisor, Dr Ting Chen Hunt, for his guidance and support throughout this research. He had patiently helped me with his extensive technical knowledge when I faced problems in my research. I am really grateful for his advice and words of encouragement.

Furthermore, I would like to thank my senior, Mr Theenagaran Subramaniam, and all my friends, for spending their precious time to support me all the time. Special thanks to SIRIM Berhad Malaysia for allowing me to use the Cold Isostatic Pressing (CIP) equipment for this research.

Lastly, I would like to express my sincere gratitude towards my family, especially my beloved grandparents, for giving me moral support during the time of difficulties. I thank God for making these to become possible.

ABSTRACT

3 mol% Ytria stabilised Tetragonal Zirconia Polycrystalline or more commonly known as 3Y-TZP, is a type of engineering ceramic Zirconia (ZrO_2). 3Y-TZP possesses outstanding mechanical properties, as well as great aesthetic value and biocompatibility. This results in 3Y-TZP to be highly demanding material in medical field market as prosthetic implant. However, one of the disadvantages of 3Y-TZP includes complication in mechanical properties caused by hydrothermal aging, which refers to spontaneous phase transformation of zirconia from tetragonal (t) into monoclinic (m) phase when it is exposed to humid condition at temperature around 65 °C to 300 °C. This condition is known as low temperature degradation (LTD). The purpose of this research is to study the effect of adding 0.2 wt% graphene additive on the mechanical properties, grain morphology and hydrothermal aging effect of 3Y-TZP at different sintering conditions. The samples were sintered at the range of 1200 °C to 1400 °C temperature, with different sintering holding time of 6 min, 1 hr and 2 hrs. The results showed that both graphene doped and undoped 3Y-TZP samples exhibited fully tetragonal phase before aging. After 12 hrs of hydrothermal aging under 180 °C, graphene doped 3Y-TZP was observed to have 0 % monoclinic contents, compared to 4.71 % of undoped 3Y-TZP, at sintering conditions of 1400 °C / 2 hrs. At sintering temperature of 1400 °C, the relative density of the 3Y-TZP samples was generally higher, with the maximum at 97.83 % relative density. Meanwhile, graphene additive improved the relative density results of 3Y-TZP at 1200 °C sintering temperature. In terms of Vickers hardness, graphene doped 3Y-TZP at sintering temperature and holding time of 1400 °C and 6 min respectively achieved the value of 14.81 GPa, highest among other samples. Furthermore, addition of graphene was discovered to be effective in improving fracture toughness of 3Y-TZP at sintering temperature of 1400 °C. SEM microstructure images revealed that addition of 0.2 wt% graphene additive did not have any effect on the grain morphology and average grain size of 3Y-TZP at sintering temperature of 1200 °C. One critical finding revealed that graphene doped 3Y-TZP at 1400 °C, 6 min sintering conditions showed promising result in terms of mechanical properties and resistance to hydrothermal aging.

TABLE OF CONTENTS

DECLARATION		i
APPROVAL FOR SUBMISSION		ii
ACKNOWLEDGEMENTS		iv
ABSTRACT		v
TABLE OF CONTENTS		vi
LIST OF TABLES		ix
LIST OF FIGURES		x
LIST OF SYMBOLS / ABBREVIATIONS		xii
LIST OF APPENDICES		xiii
CHAPTER		
1	INTRODUCTION	1
1.1	General Introduction	1
1.2	Importance of the Study	2
1.3	Problem Statement	2
1.4	Aim and Objectives	3
1.5	Scope and Limitation of the Study	3
1.6	Contribution of the Study	3
1.7	Outline of the Report	4
2	LITERATURE REVIEW	5
2.1	Introduction to Ceramic	5
2.1.1	Comparison with Metal and Polymer	5
2.2	Types of Ceramic	6
2.2.1	Application of Different Types of Ceramic	6
2.3	Review of Zirconium Dioxide	7
2.3.1	Structure and Composition of Zirconia	8
2.3.2	Different Types of Zirconia Ceramic	9
2.3.3	LTD / Hydrothermal Aging	11
2.3.4	Transformation Toughening of Zirconia	12

2.4	Zirconia as a Promising Material in Medical Field	13
2.4.1	Challenges of Zirconia in Medical Field	14
2.5	Effect of Different Additive on Y-TZP	15
2.5.1	CuO-doped Y-TZP	16
2.5.2	SS316-doped Y-TZP	16
2.5.3	GO-doped Y-TZP	18
2.5.4	GNP-doped Y-TZP	19
2.5.5	GPL-doped YSZ	21
2.6	Summary	22
3	METHODOLOGY AND WORK PLAN	24
3.1	Experiment Preparation	24
3.1.1	Powder Preparation	24
3.1.2	Powder Mixing	24
3.1.3	Green Body Preparation	25
3.1.4	Sintering	26
3.1.5	Grinding and Polishing (Disc Samples)	26
3.1.6	Thermal Etching (Disc Samples)	26
3.1.7	Hydrothermal Ageing (Bar Samples)	27
3.2	Measurement of Results	27
3.2.1	Measurement of Densification	27
3.2.2	Measurement of Vickers Hardness	28
3.2.3	Measurement of Fracture Toughness	28
3.2.4	Measurement of Monoclinic Content	29
3.3	Research Flow Chart	30
4	RESULTS AND DISCUSSION	31
4.1	XRD Phase Analysis (Pre-Aging)	31
4.2	XRD Phase Analysis (12 hrs Hydrothermal Aging)	32
4.3	Mechanical Properties Analysis	35
4.3.1	Relative Density	35
4.3.2	Vickers Hardness	36
4.3.3	Fracture Toughness	37
4.4	SEM Analysis	38
5	CONCLUSIONS AND RECOMMENDATIONS	41
5.1	Conclusions	41

5.2	Recommendations for Future Work	42
	REFERENCES	43
	APPENDICES	45

LIST OF TABLES

Table 2.1: Comparison between Metal, Polymer and Ceramic (Shabalin, 2015)	6
Table 2.2: Classification of Ceramic (Martin, 2006)	6
Table 2.3: Terminology Used to Describe Different Types of Zirconia (Hannink, Kelly and Muddle, 2004)	10
Table 2.4: Average Tetragonal Grain Size (μm) of Y-TZP of Different Graphene Oxide Content at Different Sintering Temperature (Ramesh <i>et al.</i> , 2016)	19
Table 2.5: Relative Density and Mechanical Properties Results of GNP doped 3Y-TZP (Chen <i>et al.</i> , 2015)	20
Table 3.1: Weight Composition for Doped and Undoped for One Sample	24
Table 3.2: Calculated Amount of 3Y-TZP and Graphene Powders Used for Mixing	25
Table 3.3: Actual Amount of 3Y-TZP and Graphene Powders Used for Mixing	25
Table 4.1: Monoclinic Content Percentage (%) of 3Y-TZP Samples at Different Sintering Conditions	34

LIST OF FIGURES

Figure 2.1: Three Distinct Crystal Phases: (a) Cubic (b) Tetragonal (c) Monoclinic (Hannink, Kelly and Muddle, 2004)	8
Figure 2.2: Cubic Crystal Structure (Martin, 2006)	9
Figure 2.3: Transformation Toughening Inhibits Crack Propagation in Zirconia (Martin, 2006)	13
Figure 2.4: Various Failure Modes in Zirconia Layers (Zhang and Lawn, 2019)	14
Figure 2.5: Fracture Toughness against Sintering Temperature for doped and undoped Y-TZP ceramic (Chew <i>et al.</i> , 2018)	17
Figure 2.6: Monoclinic Phase Content against Aging Duration for doped and undoped Y-TZP ceramic (Chew <i>et al.</i> , 2018)	17
Figure 2.7: Fracture Toughness against Sintering Temperature (Ramesh <i>et al.</i> , 2016)	18
Figure 2.8: Surface of 0.01 wt% GNP doped 3Y-TZP Sintered at 1300 °C [(a) Uniform Dispersion of GNP was Indicated by Arrows, (b) GNP was Shown to be Embedded in Matrix] (Chen <i>et al.</i> , 2015)	20
Figure 2.9: Relative Density (%) against GPL Content (Vol%) (Liu <i>et al.</i> , 2017)	21
Figure 2.10: Hardness (GPa) against GPL Content (Vol%) (Liu <i>et al.</i> , 2017)	22
Figure 2.11: Fracture Toughness (MPa m ^{1/2}) against GPL Content (Vol%) (Liu <i>et al.</i> , 2017)	22
Figure 3.1: Research Methodology Flow Chart	30
Figure 4.1: XRD Plot of Graphene Doped and Undoped 3Y-TZP at 1200 °C Sintering Temperature	31
Figure 4.2: XRD Plot of Graphene Doped and Undoped 3Y-TZP at 1300 °C Sintering Temperature	32
Figure 4.3: XRD Plot of Graphene Doped and Undoped 3Y-TZP at 1400 °C Sintering Temperature	32

Figure 4.4: Relative Density against Sintering Temperature and Sintering Time for 3Y-TZP	36
Figure 4.5: Vickers Hardness against Sintering Temperature and Sintering Time for 3Y-TZP	37
Figure 4.6: Fracture Toughness against Sintering Temperature and Sintering Time for 3Y-TZP	38
Figure 4.7: Microstructure Development for 3Y-TZP Samples at Sintering Temperature of 1200 °C [(a) Undoped 6 min, (b) Undoped 1 hr, (c) Undoped 2 hr, (d) 0.2 wt% Graphene Doped 6 min, (e) 0.2 wt% Graphene Doped 1 hr, (f) 0.2 wt% Graphene Doped 2 hr]	40

LIST OF SYMBOLS / ABBREVIATIONS

3Y-TZP	3 mol% Yttria doped Tetragonal Zirconia Polycrystal
c	Cubic Phase
CIP	Cold Isostatic Pressing
CuO	Copper Oxide
GNP	Graphene Nanoplatelet
GO	Graphene Oxide
GPL	Graphene Platelet
H _v	Vickers Hardness
K _{IC}	Fracture Toughness
LTD	Low Temperature Degradation
m	Monoclinic Phase
MnO	Manganese Oxide
SEM	Scanning Electron Microscope
t	Tetragonal Phase
TZP	Tetragonal Zirconia Polycrystal
XRD	X-Ray Diffraction
Y-TZP	Yttria stabilised Tetragonal Zirconia Polycrystal
ZrO ₂	Zirconia or Zirconium Dioxide

LIST OF APPENDICES

APPENDIX A: Experiment Apparatus	45
APPENDIX B: Density Chart of Water (g/cm ³) at Temperature of 0 °C to 39.9 °C	54

CHAPTER 1

INTRODUCTION

1.1 General Introduction

Among of all the types of engineering ceramic, zirconia shines the most in its outstanding mechanical properties, specifically fracture toughness. As claimed by Garvie, zirconia was revealed to have mechanical properties resemble to that of steel (Aragón-Duarte *et al.*, 2017). Ever since then, many authors had supported Garvie's claim by showing similar result while conducting research on zirconia. Research paper written by Ramesh *et al.*, (2016) had expressed agreement to the claim by stating that Ytria-tetragonal zirconia polycrystals (Y-TZP) was on high demand for medical or engineering application because of its excellent strength and good resistance to wearing. As such, zirconia is undoubtedly an excellent grade material to be applied in highly sophisticated situation. Nevertheless, some researcher suggested that zirconia is still far from being perfect. A perfect example to illustrate the statement was suggested by Schünemann *et al.*, (2019) in their research paper which revealed that there were some controversies toward zirconia as prosthesis due to high number of failures involving zirconia based material being reported.

On the other hand, numerous researches had been carried out by adding additives to zirconia ceramic. Some of the additives were graphene-based, such as graphene oxide (GO), graphene platelet (GPL) and graphene nano-platelet (GNP). Originally, graphene consists of carbon element and its uniqueness lies in its thin layer, yet it has displayed great mechanical properties. Some researcher suggested that the addition of graphene into engineering ceramic will contribute to the improvement of mechanical properties of engineering ceramic (Boniecki *et al.*, 2017). One of the notable mentions of successful research was conducted by Ramesh *et al.* (2016) The authors discovered that 0.2 wt% graphene oxide (GO) doped Y-TZP specimens achieved remarkable fracture toughness at sintering temperature of 1400 °C, in comparison with undoped Y-TZP. Their study gave rise to countless possibilities of future research on the subject of graphene additive to zirconia ceramic.

1.2 Importance of the Study

Zirconia is an engineering ceramic material which has gained reputation over the years in medical field. As proven by several researchers in their studies, zirconia may be a material capable of dominating the market in the future of medical field. In a paper written by Naveau, Rignon-Bret and Wulfman (2019), they claimed that the rise of zirconia as popular choice was contributed by its aesthetics value. The gingival appearance of zirconia had enabled this material to have better colour integration as abutments for dental patients. Sivaraman *et al.* (2018) claimed that this engineering ceramic was a possible material to replace titanium as implant systems in patient's oral. Zirconia had significant advantages in soft-tissue response, biocompatibility and aesthetics compared to titanium. With further research, the zirconia may be able to prevail as 'first choice' material in medical field, especially dentistry.

Aside from medical field, zirconia has many other applications in engineering industries as cutting tool, refractory, heat engine, oxygen sensors and electrolytes in fuel cells. It is worth to know that the excellent mechanical properties and chemical inertness as well as high thermal resistance of zirconia enable it to sustain under long term application. Further enhancement of zirconia in terms of mechanical properties will increase the involvement of this engineering ceramic in various application.

1.3 Problem Statement

Despite possessing great mechanical properties among other engineering ceramics, zirconia is still inferior compared to metals such as titanium and steel. Several authors in the journal of "Zirconia surface modifications for implant dentistry" suggested that currently zirconia is unable to replace titanium as first choice material for dental or another medical implant application. This is mainly caused by complications in mechanical strength of zirconia and resulted in higher probability of failure over time (Schünemann *et al.*, 2019).

Another major issue to be considered is the hydrothermal aging effect of zirconia. Hydrothermal aging refers to the spontaneous phase transformation of zirconia from tetragonal (t) into monoclinic (m) phase when it is exposed to humid condition at temperature around 65 °C to 300 °C. This transformation is fatal to zirconia as it will lead to degradation of mechanical properties, known

as low temperature degradation (LTD) (Ramesh *et al.*, 2016). After the discovery of LTD, many researchers had put in effort to study the factors governing the LTD, with the hope to eradicate this issue.

1.4 Aim and Objectives

In the current research, the aim is to investigate influence of graphene on the mechanical properties and aging resistance of 3 mol% Ytria stabilised Tetragonal Zirconia Polycrystals (3Y-TZP) at different sintering conditions. In order to achieve the aim, the following aspects will be focused on:

1. To compare the dissimilarity between graphene doped and undoped 3Y-TZP in terms of mechanical properties and grain morphology.
2. To study the effects of sintering holding time and temperature on the mechanical properties of graphene doped 3Y-TZP.
3. To identify the sintering condition for 3Y-TZP with good hydrothermal aging resistance.

1.5 Scope and Limitation of the Study

The type of zirconia that will be used is 3Y-TZP. The research is limited to the use of only one type of dopant, which is graphene, at the concentration of 0.2 wt%. Two different shapes of samples will be produced, which are bar sample and disc sample. The sintering temperature will be adjusted to a temperature range of 1200 °C to 1400 °C. Meanwhile, the sintering holding time will vary between 6 minutes, 1 hour and 2 hours. The sintered sample will be evaluated in terms of mechanical properties, specifically the fracture toughness and densification. Resistance of sintered samples to hydrothermal aging will be measured in terms of the percentage of phase transformation to monoclinic with respect to time.

1.6 Contribution of the Study

The study on 3Y-TZP zirconia is mostly favourable to medical field due to the high demand of prosthetic. Other than that, zirconia has many other applications in engineering industries. Over the years, researchers had been experimenting with 3Y-TZP by adding various additives such as CuO, GO and SS316 with the hope to further improve its mechanical properties and resistance to

hydrothermal aging. Current research is expected to study whether 0.2 wt% graphene is a suitable additive which could be beneficial to 3Y-TZP, under different sintering conditions.

1.7 Outline of the Report

As an overall view, this report consists of a total of five chapters which includes introduction, literature review, methodology, results and conclusion.

Chapter 1 presents a glimpse to the engineering ceramic zirconia, which is the main subject of this research. This chapter discusses about the rise of zirconia in medical field, significance of zirconia in various application, the problem faced by zirconia and finally the aim and scope of the research.

Chapter 2 reviews the introduction to ceramic, followed by the introduction to engineering ceramic. The structure and properties of zirconia as a part of engineering ceramic is also revealed, along with its weaknesses. In addition, the potential and challenges of zirconia in medical field is also discussed. This chapter ends with the effect of sintering on graphene-doped Y-TZP.

Chapter 3 focuses on the procedures involved in preparing the samples for the research. Furthermore, this chapter also elaborates the theoretical methods for mechanical properties evaluation, as well as the methods for microstructure and phase composition analysis.

Chapter 4 discusses the result obtained from this research. The comparison between graphene doped and undoped 3Y-TZP is made in the aspect of mechanical properties, phase analysis, hydrothermal aging resistance, microstructure and average grain size. In the meantime, this section also examines the behaviour of 3Y-TZP samples when it is subjected to various sintering conditions.

Chapter 5 concludes the finding of the whole research as well as some useful recommendation for the next research.

CHAPTER 2

LITERATURE REVIEW

2.1 Introduction to Ceramic

From the historical point of view, the word ‘ceramic’ was derived from Greek word. Originally, it means ‘pottery’. It refers to domestic wares as well as art objects which are clay-based and widely known by mankind as daily life object. In today’s standard, the term ‘ceramic’ has evolved to include materials such as glass, cement and advanced engineering ceramic (Shabalin, 2015).

According to the author Shabalin (2015), ceramic or ceramic materials are known as solid compositions which are produced by involving the usage of high temperature and high pressure. Ceramic consist of at least one non-metallic chemical element. In comparison to other type of materials, ceramic can be easily distinguished by having special characteristics of high melting point, brittle and non-reactive nature.

In addition, ceramic is also a common term used to define materials that are used in daily life such as glass, tiles, pottery, porcelain, bricks and cement. This is due to the “refractory” characteristic of the materials. In other words, they have the characteristic of being durable while performing in high temperature, acids, wear and tear and other extreme condition. Similarly, engineering ceramic also falls in the same category (Woodford, 2019).

2.1.1 Comparison with Metal and Polymer

Shabalin (2015) explained that there are different types of bonding mechanism which normally co-exist in the same phases in ceramic, namely, ionic bond, covalent bond, and metallic bond. These contributes to the unique properties of ceramic. On the other hand, metal is only dominant in metallic bonding, while polymer only prevails in covalent bonding. Table 2.1 shows the difference between ceramics, metals and polymers in terms of properties.

Table 2.1: Comparison between Metal, Polymer and Ceramic (Shabalin, 2015)

Properties	Metal	Polymer	Ceramic
Melting point	Low to high	Low	High
Density	Medium to high	Very low	Low
Elastic Modulus	Medium to high	Low	Very high
Plasticity	Ductile	Ductile to brittle	Brittle
Chemical Stability	Reactive	Very reactive	Non-reactive

2.2 Types of Ceramic

Ceramic materials in general can be categorised into three groups, which are summarised in Table 2.2 below:

Table 2.2: Classification of Ceramic (Martin, 2006)

Natural Ceramic	Domestic Ceramic	Engineering Ceramic
Available in the form of stone such as limestone and granite.	Created through clays.	Produced from nitrides, oxides or carbides.
Oldest type of construction material.	Examples are pottery, porcelain, refractory bricks and tiles.	Enhanced strength and toughness.
-	Up to 20% porosity and many microcracks.	Smaller microcracks.

As summary, engineering ceramics are engineered for highly specific application due to their improved properties, unlike domestic ceramics which are more on general purpose.

2.2.1 Application of Different Types of Ceramic

The application of ceramics mainly depending on their properties. For instance, domestic ceramics such as glass ceramics are produced as cookware, bakeware and cooktops due to their properties of low co-efficient of thermal expansion

and good resistance to thermal shock. On top of that, clay is a natural occurring ceramic which consist of elements silicon, aluminium and oxygen. After a few processing methods which include cutting, moulding, and firing, the clay could be turned into hard bricks. These bricks are typically applied in two common areas, which are building and refractory. These applications are correlated with the durability and high temperature resistance properties of brick (Woodford, 2019).

Engineering ceramics are more advanced type of ceramics. Basically, these materials tend to have a higher tier of properties compared to domestic and natural ceramics. Engineering ceramic are well established in a more specific application by engineers such as neutron moderator in fission reactor, heating elements and electrodes for furnaces, high temperature furnace lining, thermal protection for aerospace, anticorrosion protection for chemical equipment (Shabalin, 2015). In medical field, engineering ceramics especially alumina and zirconia play an important role as prosthesis for knee replacement, dental implants and many other orthopaedic operations. They are chemically inert and hard, which enable them to be the perfect material for the situation.

2.3 Review of Zirconium Dioxide

Zirconium dioxide (ZrO_2), or more commonly named as zirconia, is a subset of engineering ceramic and is the focus of this research. Zirconia is a product of combination between zirconium element and oxygen element. Pure zirconium has the appearance of white and ductile metal in crystalline form while it appears as blue-black powder in amorphous form. This element Zr only occur in as silicates oxides or as free oxides (ZrO_2). Hence, it is nearly impossible to find Zr element in its pure state. Zirconium dioxide, however, can be identified with the appearance of white crystalline oxide (Abd El-Ghany and Sherief, 2016).

As suggested by Garvie, zirconia was referred as “ceramic steel” due to its properties which are similar to those of steel (Aragón-Duarte *et al.*, 2017). The origin of “Zirconium” name was derived from Arabic word “Zargon” which bear the meaning of “golden in colour”. Meanwhile, Martin Heinrich Klaproth, a German chemist, had accidentally discovered this compound ZrO_2 in 1789 during his work which involved heating of some gems. Ever since then, ZrO_2 had been applied in various field, including medical field as biomaterials. The

first usage of ZrO_2 as biomaterial was in 1969. It was used in orthopaedic as an alternative material for hip head replacement (Abd El-Ghany and Sherief, 2016).

2.3.1 Structure and Composition of Zirconia

Zirconia is an engineering ceramic which exhibits three distinct crystal phases with respect to temperature:

- i) Cubic crystal structure at temperature above 2300 °C,
- ii) Tetragonal crystal structure at temperature between 1150 °C and 2300 °C,
- iii) Monoclinic crystal structure at temperature below 1150 °C.

The crystal phases are illustrated in Figure 2.1. It is worth to note that the cubic phase (C) has the shape of square sides straight prism, while tetragonal phase (T) appears in the shape of rectangular sides straight prism. Meanwhile, monoclinic phase (M) is in the shape of a deformed prism with parallelepiped sides. These differences in the shape are resulted from the huge temperature differences. In terms of mechanical properties, tetragonal phase prevails with the enhanced properties, followed by cubic phase with moderate properties and lastly monoclinic phase with lower properties which may cause reduction of ceramic particle cohesion (Abd El-Ghany and Sherief, 2016).

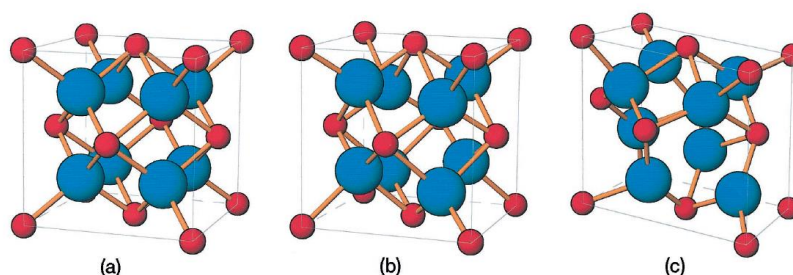


Figure 2.1: Three Distinct Crystal Phases: (a) Cubic (b) Tetragonal (c) Monoclinic (Hannink, Kelly and Muddle, 2004)

Based on illustration in Figure 2.2, empty holes in the zirconia structure are inhabited by oxygen ions. On top of that, zirconium ions are positioned in face-centred cubic (FCC) lattice. Another fact to add is that zirconia experiences volume expansion up to 3.5 % during cooling below 1000 °C. This is resulted

from the change in crystal structure when the temperature decreases and will lead to failure of material (Martin, 2006).

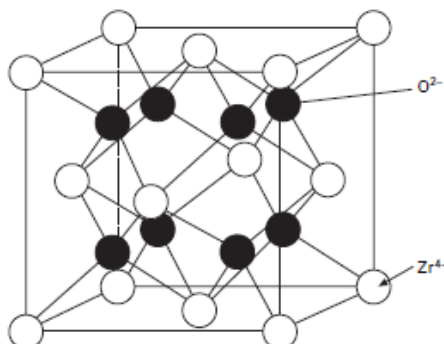


Figure 2.2: Cubic Crystal Structure (Martin, 2006)

Furthermore, a journal article by Abd El-Ghany and Sherief (2016) suggested that change in volume from cubic (c) phase to tetragonal (t) phase is approximately 2.31 % and roughly 4.5 % upon decreasing of temperature. Volume changes on cooling from tetragonal (t) phase monoclinic (m) phase will then contribute catastrophic failure. This causes the material to become unpractical for applications which demand a durable and rigid structure. Nevertheless, the transformation is reversible.

On the other hand, addition of CaO, Y₂O₃ or MgO to the zirconia will enhance the stability of cubic crystal structure over the temperature range, and the phase transformation will cease from occurring. This addition will result in the formation of stabilised zirconia. Stabilised zirconia however, will have poor resistance to impact as well as low fracture toughness. (Martin, 2006).

2.3.2 Different Types of Zirconia Ceramic

Zirconia in its pure state has infeasible application for structural ceramic since it experiences phase transformation during cooling from high temperature to below 1150 °C. The transformation is accompanied by expansion in volume which will later on cause instability in structure. Hence, manufacturing of the material is highly not recommended (Aragón-Duarte *et al.*, 2017). In addition, this fact is also supported by Abd El-Ghany and Sherief (2016) in their journal article which states that pure zirconia is unpractical for usage due to the probability of catastrophic failure during volume expansion.

Suggested solution to the problem above is to stabilise zirconia with other oxides. Some examples of the oxides is yttria, which stabilises total or partially with tetragonal and cubic phase of zirconia, and results in Yttrium Tetragonal Zirconia Polycrystals (Y-TZP) (Aragón-Duarte *et al.*, 2017). Other types of zirconia ceramic and their terminology are listed in Table 2.3:

Table 2.3: Terminology Used to Describe Different Types of Zirconia (Hannink, Kelly and Muddle, 2004)

Zirconia Type	Description
DZC	Dispersed zirconia ceramics.
MPZ	Monoclinic polycrystalline zirconia.
PSZ	Partially stabilised zirconia.
Ca-PSZ	Calcium-cation-doped PSZ.
CaO-PSZ	
Mg-PSZ	
MgO-PSZ	Magnesium-cation-doped PSZ.
TTA	Transformation-toughened alumina.
TTC	Transformation-toughened ceramics.
TTZ	Transformation-toughened zirconia.
TZP	Tetragonal zirconia polycrystals.
Y-TZP	Yttrium-cation-doped tetragonal zirconia polycrystals.
ZTA	Zirconia toughened alumina.
ZTC	Zirconia toughened ceramics.

Y-TZP usually contain 3 mol% of yttria (Y_2O_3) as stabiliser, therefore it is more common to be named as 3Y-TZP. This specific type of zirconia has been used to fabricate femoral heads for the purpose of hip replacement prostheses. Furthermore, it is also applied in dentistry for the manufacturing of dental crowns. As good as it looks, it has mechanical properties of 900-1200Mpa flexural strength as well as $9-10Mpa(m)^{1/2}$ fracture strength. Grain size plays an important role in affecting the mechanical properties of 3Y-TZP. Other than that, sintering is a method to alter grain size, thus, it can indirectly contribute to both stability and strength of 3Y-TZP. Different sintering condition such as high

temperature and long sintering time will eventually result in larger grain size and vice versa.

Meanwhile, ZTA is another type zirconia which has addition of alumina matrix. It is produced through soft machining or slip casting, followed by sintering. ZTA is a porous composite ceramic which comprise between 8 and 11 % in terms of porosity. ZTA has larger amount of porosity in comparison with 3Y-TZP. As result, ZTA has lower mechanical properties compared to 3Y-TZP.

Mg-PSZ in general has a large amount of porosity, in addition to large grain size between 30-60 μ m which in turn leads to low overall mechanical properties and low stability. Moreover, it is not an easy task to achieve Mg-PSZ compounds free of silicone dioxide. This is because, the silicon dioxide will react with the magnesium in Mg-PSZ to form Magnesium Silicates. If that happens, the concentration of Mg in the Mg-PSZ will decrease and this will encourage (T) to (M) transformation. This will further reduce the stability and mechanical properties of Mg-PSZ (Abd El-Ghany and Sherief, 2016).

2.3.3 LTD / Hydrothermal Aging

Low Temperature Degradation (LTD) is a phenomenon where the mechanical properties of zirconia deteriorate when the material is being exposed to hydrothermal aging. Hydrothermal aging refers to humid environment at temperature of 100 °C to 300 °C. This condition of hydrothermal aging results in phase transformation of zirconia from tetragonal to monoclinic at low temperature (Ramesh, Lee and Tan, 2018).

Swab (1991), suggested in his article that there are six characteristics of LTD in zirconia which can be observed. The first characteristic explained that LTD occurs frequently at temperature between 200 °C to 300 °C. The second characteristics discussed that LTD will lead to lower mechanical properties of zirconia (strength, toughness and density). The third characteristics suggested that LTD is caused by tetragonal to monoclinic phase transformation along with microcracking. The fourth characteristics talked about the phase transformation which will commonly initiates at the surface. The fifth characteristic explained that the higher rate of phase transformation is due to the presence of water, hence

the term hydrothermal aging. The sixth characteristics involved the relationship between LTD and grain size or stabiliser content.

Ramesh, Lee and Tan (2018) has further proven the article suggested by Swab (1991) by pointing out that there are various factors governing hydrothermal aging of zirconia (Y-TZP) which includes grain size, sintering technique, starting powder, yttria content, addition of dopants or sintering additives and ageing environment (humidity and low temperature).

Condition of LTD had brought a negative impact to development of zirconia. For instance, steam sterilization of zirconia femoral heads had led to failure of hip prostheses between 1999 to 2000. The presence of humid environment through steam sterilization caused increased wear on acetabular component. As consequence, usage of zirconia as hip prostheses in the market had significantly reduced. On the bright side, researchers had been trying to rectify the LTD condition in zirconia over the past decade by manipulating the factors influencing LTD behaviour of zirconia (Ramesh, Lee and Tan, 2018).

2.3.4 Transformation Toughening of Zirconia

The term transformation toughening of zirconia was initiated by Garvie, Hannink and Pascoe in their research paper. The fundamental principle of transformation toughening involves controlled phase transformation of tetragonal to monoclinic. This transformation allows zirconia to exhibit enhanced mechanical properties (Hannink, Kelly and Muddle, 2004).

The mechanism of transformation toughening can be observed in Figure 2.3. Ramesh *et al.* (2016) had provided some insight regarding the mechanism of transformation toughened zirconia. In their journal, they stated that metastable tetragonal grain of transformation toughened zirconia will absorb a stress created by a propagating crack. The metastable tetragonal grain will then transform into monoclinic symmetry after absorbing stress. This phenomenon will lead to a slight volume expansion that will produce compressive stress around crack tip. In short, higher strength should be applied to allow the crack to propagate further because transformation toughened zirconia inhibits the crack propagation.

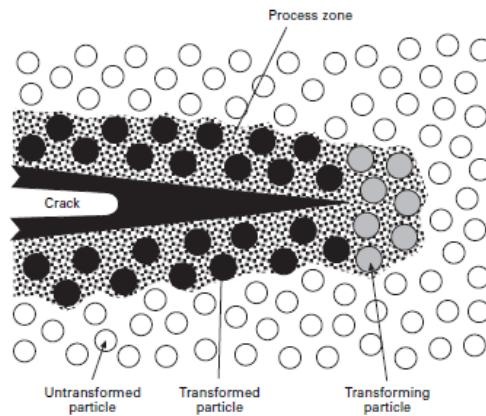


Figure 2.3: Transformation Toughening Inhibits Crack Propagation in Zirconia (Martin, 2006)

2.4 Zirconia as a Promising Material in Medical Field

Osseointegration concept was first discovered in 1908 by Branemark when blocks of titanium was placed into the femur of rabbit. He made an impactful discovery when he realised that the titanium could not be retrieved from the rabbit and was tightly attached with the surrounding bone. From that moment onwards, numerous clinical studies had been performed and proved that titanium was a reliable biomaterial for prosthetic rehabilitation. Following the success of titanium, various modification had been made to improve its physical, optical and mechanical properties. This was done by reviewing the design of implant, the structure as well as composition of the material.

Despite the continuous study and enhancement, a number of inherent flaws still persisted in titanium. Titanium had been criticised for causing undesirable allergic reactions, galvanic current formation, cellular sensitization to the patient. Furthermore, the aesthetics gray hue of titanium did not look appealing to the consumer. Following this matter, the search for more aesthetics and biocompatible implant continued due to its demands (Sivaraman *et al.*, 2018).

The success of an implant material is depending on its mechanical properties and aesthetic value. Zirconia is a ceramic-based material which has been selected as a promising material for osseointegration and implant due to its appearance (Naveau, Rignon-Bret and Wulfman, 2019). Coincidentally, zirconia-based material is also claimed to have a high chemical stability which would avoid the release of toxin to the surrounding tissue and cause

inflammation or damage in tissue to the patient. In fact, 3Y-ZTP is able to provide simulation of osteogenic cell on top of having high affinity to bone tissue compared to most biocompatible ceramics. Recent studies had identified both zirconia and titanium implants have similar results regarding osseointegration indexes. In spite of the studies done, zirconia as implant still prevails over titanium in the aspect of aesthetic, since corrosion and greyish colour of titanium contributes to its disadvantages. In addition, zirconia is shown to have the ability to decrease bacteria adhesion and biofilm accumulation. These advantages enable zirconia to provide low risk of inflammatory in surrounding tissues of implant (Schünemann *et al.*, 2019).

2.4.1 Challenges of Zirconia in Medical Field

Despite of all the advantages zirconia possesses, this material is not entirely immune to failure over time. Prostheses such as bridges and crowns are frequently subjected to high load under repeated condition in watery environments. Under normal circumstances, bite force of an average human can exceed 1000N of force, and it occurs continuously throughout the lifetime contact event of 10^6 . As shown in Figure 2.4, the probability of clinical failure in zirconia is a crucial factor to be acknowledged given that new generation of this material tends to be more translucent for the sake of aesthetic, but with potentially limited strength and toughness (Zhang and Lawn, 2019).

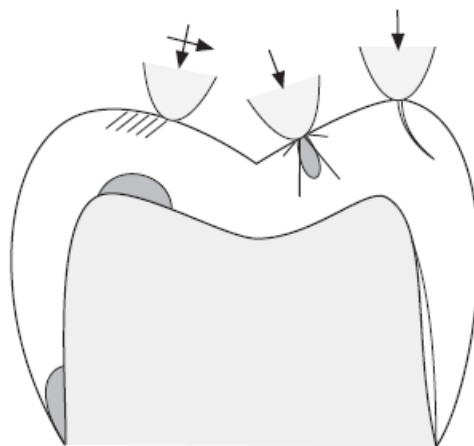


Figure 2.4: Various Failure Modes in Zirconia Layers (Zhang and Lawn, 2019)

Another challenge faced by zirconia is that it suffers from lack of mechanical strength due to technical complications. This has demoted zirconia as first choice implant material following its complication. Currently, the leading material for dental implant is still titanium, due to it having higher mechanical strength over zirconia for the dental or other implant application (Schünemann *et al.*, 2019). The problem is further confirmed by Naveau, Rignon-Bret and Wulfman (2019) in their journal article, which also claimed that titanium abutments had lesser mechanical complications than zirconia abutments. In addition, mechanical complication of zirconia reported in the study by Naveau, Rignon-Bret and Wulfman (2019) showed no changes over the past five years.

In conclusion, studies had demonstrated that zirconia implants might be a promising alternative to titanium with its advantage in biocompatibility, osseointegration, aesthetic, as well as soft tissue response (Sivaraman *et al.*, 2018). However, thorough research should be conducted in the aspect of structural and composition as well as the influence of additive on the properties of zirconia in order to eliminate or reduce the mechanical complication, so that it can be on par with titanium implants.

2.5 Effect of Different Additive on Y-TZP

To date, numerous researches had been conducted out in an effort to reduce the weaknesses found in Y-TZP. Ramesh and Gill (2001) had carried out a research by using copper oxide (CuO) as additive on Y-TZP. Chew, Matthew and Ramesh (2018) conducted similar research by using SS316 stainless steel of 0.1 wt% to 1 wt% as dopant.

The usage of graphene-based dopant in Y-TZP had also been carried out as a part of research. Boniecki *et al.* (2017) discovered that addition of 0.02 wt% of graphene oxide (GO) to Y-TZP under sintering of 1400 °C for 1h would increase the fracture toughness by 42 % compared to undoped Y-TZP. In addition, Ramesh *et al.*, (2016) conducted a research by using GO doped Y-TZP at varying GO amount up to 1 wt%, as well as varying sintering temperature up to 1500 °C in order to study densification, mechanical properties and effect on LTD. The authors discovered that doped Y-TZP had improved densification and high fracture toughness in comparison with undoped Y-TZP at low sintering

temperature of 1200 °C. Unfortunately, GO additive was found to be ineffective in suppressing the LTD effect of Y-TZP.

Even though there are other journal reports by Liu *et al.* (2017), Obradovi and Kern (2018) as well as Chen *et al.* (2015) which utilised graphene platelets (GPL) and graphene nanoplatelet (GNP) as dopants, but the studies of graphene dopant on 3Y-TZP at different sintering holding time had yet to be explored.

2.5.1 CuO-doped Y-TZP

The usage of copper oxide (CuO) additives on Y-TZP was conducted by Ramesh and Gill (2001) in their research entitled “Environmental Degradation of CuO doped Y-TZP”. The main purpose of their research was to study the benefits of adding CuO dopants on the LTD resistance and the mechanical properties of Y-TZP, under sintering duration of 2 hours at 1300 °C.

The results obtained were astonishing, as the mechanical properties of CuO doped Y-TZP samples were generally higher compared to pure Y-TZP. One of the results revealed that sintering 0.05 wt% copper oxide (CuO) doped Y-TZP at temperature of 1300 °C for two hours had shown high fracture toughness ($>19 \text{ MPa m}^{1/2}$) while at the same time exhibited good aging resistance compared to undoped Y-TZP. It was believed that addition of small percentage of CuO was be able to tackle LTD issue of Y-TZP without compromising with the mechanical properties, even though further studies were still necessary.

2.5.2 SS316-doped Y-TZP

A research had been conducted by Chew, Matthew and Ramesh (2018) to address the problem faced by Y-TZP in medical field. Prior to the research, numerous cases which include failure of hip transplant had been reported and discovered that the root of the problem was due to material Y-TZP. In this research, Stainless Steel 316 (SS316) was selected to be doped with Y-TZP with the purpose to study the changes in mechanical properties. Other factor such as sintering condition was also taken into consideration during the research. At the end of the research, this metal-doped zirconia material was expected to have enhanced strength and durability compared to pure zirconia. This was because,

stainless steel by itself had displayed excellent toughness and strength in addition to high resistance to corrosion.

Figure 2.5 and Figure 2.6 show the results of the experiment in terms of fracture toughness and LTD. As summary, 0.1 wt% SS316 produced promising outcome due to having low monoclinic phase content with respect to aging hour. In terms of mechanical properties, 1 wt% SS316 exhibited fracture toughness of 6 MPa m^{1/2} under sintering temperature of 1300 °C and holding time of 2 hr, which exceeded fracture toughness of undoped Y-TZP (5.5 MPa m^{1/2}).

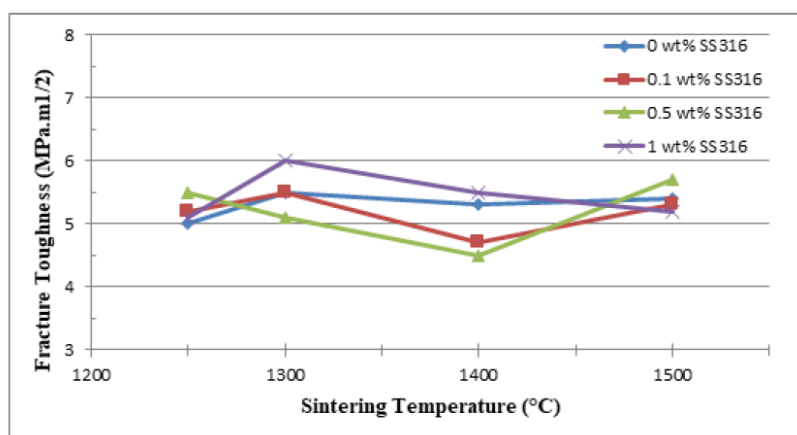


Figure 2.5: Fracture Toughness against Sintering Temperature for doped and undoped Y-TZP ceramic (Chew *et al*, 2018)

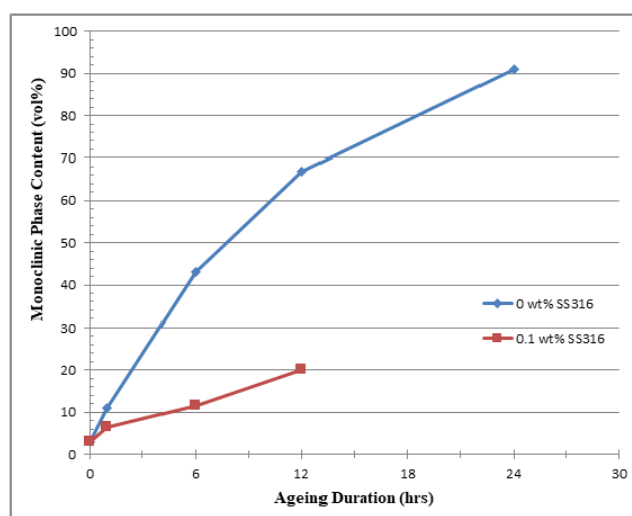


Figure 2.6: Monoclinic Phase Content against Aging Duration for doped and undoped Y-TZP ceramic (Chew *et al*, 2018)

2.5.3 GO-doped Y-TZP

Over the years, several researches had been conducted by utilizing graphene-based dopant on zirconia ceramic. Originally, graphene is made up of carbon and its uniqueness lies in its thin layer, which is as thick as the size of one atom. It is believed that the addition of graphene into ceramic will contribute to the improvement of mechanical properties of Y-TZP. This is because, graphene by itself is a material which has displayed great mechanical properties (Boniecki *et al.*, 2017). The type and composition of graphene should be considered thoroughly in the research. The research conducted by Ramesh *et al.* (2016) can be observed in Figure 2.7 below. All the samples were sintered via pressureless sintering. It was discovered that 0.2 wt% graphene oxide (GO) doped Y-TZP specimens achieved greatest fracture toughness at sintering temperature of 1400 °C.

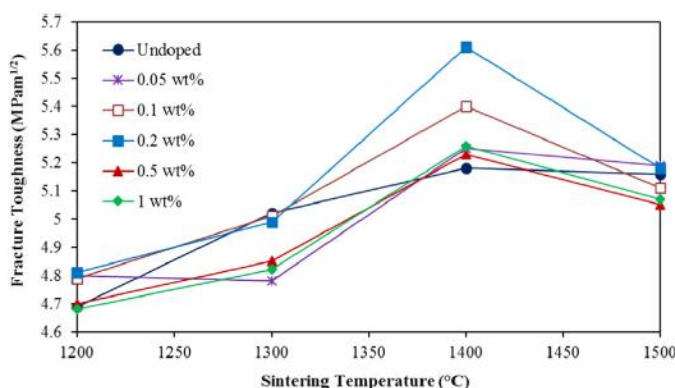


Figure 2.7: Fracture Toughness against Sintering Temperature (Ramesh *et al.*, 2016)

Aside from graphene dopant concentration, it was well documented that sintering conditions were the other factors which will alter the properties of Y-TZP. By observing Figure 2.7 shown above, the fracture toughness did not remain constant upon changes in sintering temperature. Furthermore, the result showed that at sintering temperature of 1400 °C, most of the Y-TZP samples exhibited relatively high fracture toughness compared to other temperatures. On the other hand, Table 2.4 provides another observation on how the sintering temperature would affect the grain size of Y-TZP.

Table 2.4: Average Tetragonal Grain Size (μm) of Y-TZP of Different Graphene Oxide Content at Different Sintering Temperature (Ramesh *et al.*, 2016)

GO content	Sintering temperature			
	1200 °C	1300 °C	1400 °C	1500 °C
Undoped	0.29	0.4	0.47	0.68
0.05 wt%	0.28	0.36	0.48	0.66
0.1 wt%	0.28	0.37	0.49	0.65
0.2 wt%	0.3	0.37	0.48	0.65
0.5 wt%	0.29	0.38	0.46	0.67
1 wt%	0.28	0.41	0.46	0.69

Sintering conditions can be either manipulated by temperature or time. Most of the studies conducted involve the adjustment of temperature within a range. Currently, there are not much research conducted to investigate on how the sintering holding time will affect the condition of graphene doped and undoped Y-TZP. Long sintering holding time will often result in Y-TZP samples which are more susceptible to LTD effect because of the large grain size being formed. Hence, it can be inferred that shorter sintering holding time will results in smaller grain size with improved LTD resistance.

2.5.4 GNP-doped Y-TZP

A research by Chen *et al.* (2015) was conducted by using graphene nanoplatelets (GNPs) powder as additive to enhance the properties of 3Y-TZP. The sintering method used was field assisted sintering technology (FAST), at the sintering temperature of 1200 °C to 1400 °C. The uniqueness of FAST sintering lies within the presence of uniaxial pressure, as opposed to pressureless sintering.

The outcome of their research is shown in Table 2.5. 3Y-TZP with GNP content of 0.01 wt% exhibited highest relative density and fracture toughness, but the values dropped as the GNP content increased to 0.05 wt%. This showed that the increase in relative density and fracture toughness were not proportional to the increase in GNP content. On the other hand, Table 2.5 also showed that sintering temperature played a major role in affecting the relative density and mechanical properties of 3Y-TZP. It was shown that 0.01 wt% GNP doped 3Y-TZP at sintering temperature of 1200 °C had the highest hardness value, while

at sintering temperature of 1300 °C, the sample had highest relative density and fracture toughness.

Table 2.5: Relative Density and Mechanical Properties Results of GNP doped 3Y-TZP (Chen *et al.*, 2015)

Graphene (wt. %)	Temperature (°C)	Relative density (%)	Hardness (GPa)	Fracture toughness (MPa·m ^{1/2})
0	1200	97.5	11.36	8.9
0	1300	99.2	12.46	9.5
0	1400	99.1	10.95	9.0
0.01	1200	98.9	13.56	11.2
0.01	1300	99.4	12.33	15.3
0.01	1400	99.3	12.69	9.3
0.03	1300	99.2	12.58	13.5
0.05	1300	98.9	13.02	10.5

Furthermore, the research conducted by Chen *et al.* (2015) included SEM analysis, as shown in Figure 2.8 below. The authors explained that the GNPs were shown to be dispersed uniformly across the 3Y-TZP matrix from the SEM images. The dispersion of GNP in uniform manner had indicated that the grain boundary of 3Y-TZP was strengthened significantly by inhibiting the propagation of cracks across the grain. In addition, the porosity of the 3Y-TZP was reduced, leading to enhanced relative density.

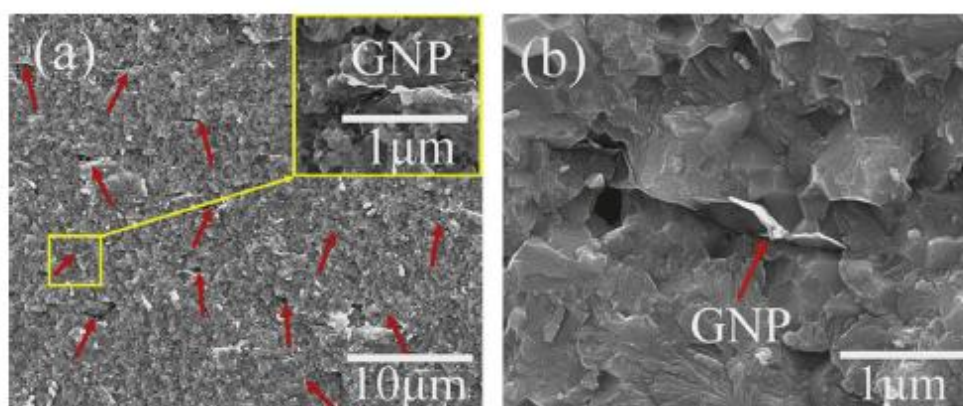


Figure 2.8: Surface of 0.01 wt% GNP doped 3Y-TZP Sintered at 1300 °C [(a) Uniform Dispersion of GNP was Indicated by Arrows, (b) GNP was Shown to be Embedded in Matrix] (Chen *et al.*, 2015)

In conclusion, the authors claimed that the GNP doped 3Y-TZP showed promising result in the aspect of fracture toughness. This statement had further proven the necessity to conduct further researches with the intention to use graphene-based material as additive for 3Y-TZP.

2.5.5 GPL-doped YSZ

The research by Liu *et al.* (2017) had provided some interesting insight regarding the usage of graphene-based additive on zirconia composites. In their research, the authors used graphene platelet (GPL) as dopant on yttria stabilised zirconia (YSZ). Similar to Y-TZP, YSZ is another type of ceramic under the subset zirconia engineering ceramic. The type of sintering used in the research was spark plasma sintering, at temperature of 1450 °C.

Figure 2.9 below shows the relative density of the samples against the content of GPL. At low percentage of GPL content, the samples showed remarkable result in relative density. On the other hand, Figure 2.10 and Figure 2.11 show the graph of samples' hardness and fracture toughness respectively. As an overall view, the authors concluded that there were noticeable enhancements of 7 % in hardness and 60 % in toughness in doped samples compared to the pure YSZ samples. Liu *et al.* (2017) claimed that the presence of small amount of GPL in YSZ had introduced the reinforcing effect as well as pull out and crack bridging to the zirconia composite, hence improving both hardness and fracture toughness significantly.

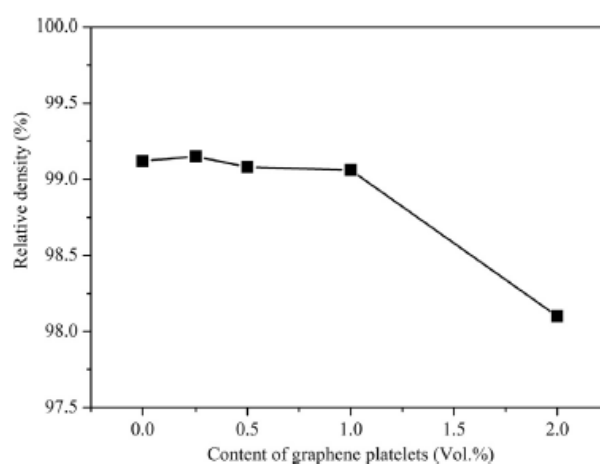


Figure 2.9: Relative Density (%) against GPL Content (Vol%) (Liu *et al.*, 2017)

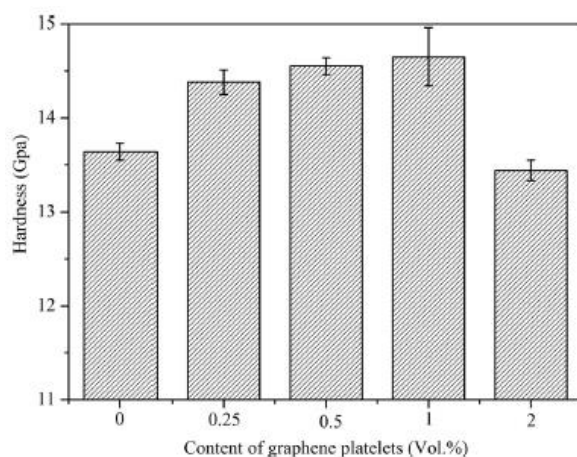


Figure 2.10: Hardness (GPa) against GPL Content (Vol%) (Liu *et al.*, 2017)

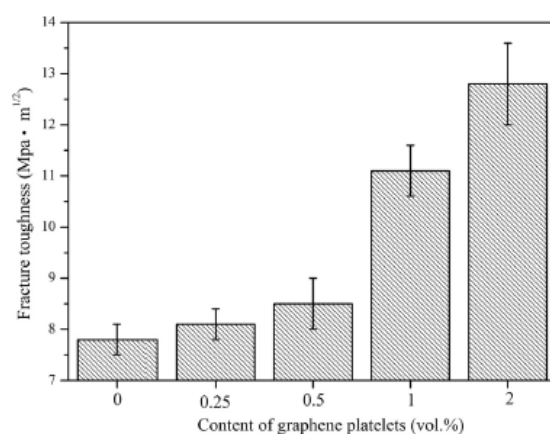


Figure 2.11: Fracture Toughness (MPa m^{1/2}) against GPL Content (Vol%) (Liu *et al.*, 2017)

The research by Liu *et al.* (2017) had opened up numerous possibilities of future research on the subject of graphene additive to zirconia ceramic. It would be interesting to work on different sintering conditions such as sintering temperature and sintering holding time, for a more in-depth study. On the other hand, the study on the resistance of doped YSZ samples to LTD effect would definitely provide another understanding on this topic. The contribution of these researches would most likely fall on engineering application, as claimed by the authors themselves at the end of their journal.

2.6 Summary

The successful research on graphene-based material by several researches had established a clear foundation on the benefits of graphene

additive in zirconia ceramic. This is especially highlighted in the significant improvement of fracture toughness, such as in the recent study of Liu *et al.* (2017). However, most of their studies stressed on the variation of additive amount rather than sintering condition.

In present work, the research would focus more on the differences of sintering conditions, especially sintering temperature and sintering holding time. Meanwhile, the graphene additives content in this research will be fixed at 0.2 wt%, because it could be observed from the research of Ramesh *et al.* (2016) that graphene doped Y-TZP at 0.2 wt% had been proved to achieve remarkable fracture toughness.

CHAPTER 3

METHODOLOGY AND WORK PLAN

3.1 Experiment Preparation

The samples preparation is divided into four major segments, which include powder preparation, powder mixing, green body preparation and sintering.

3.1.1 Powder Preparation

For this research, 3 mol% Ytria-Stabilised Tetragonal Zirconia Polycrystalline (3Y-TZP) was prepared in powder form. The 3Y-TZP powder was obtained from TOSOH, Japan. As for the dopant, 0.2 wt% of graphene powder was used. Graphene-based additive of 0.2 wt% had been proven to be the optimum weight percentage for achieving high fracture toughness when it was doped in 3Y-TZP under sintering temperature of 1400 °C (Ramesh *et al.*, 2016). There were two types of samples formed from these powders, namely undoped 3Y-TZP and graphene-doped 3Y-TZP. Table 3.1 summarised the weight composition of doped and undoped 3Y-TZP for one sample.

Table 3.1: Weight Composition for Doped and Undoped for One Sample

Sample	Bar (3g)		Disc (2.5g)	
	Weight of 3Y-TZP (g)	Weight of Graphene (g)	Weight of 3Y-TZP (g)	Weight of Graphene (g)
Undoped Y-TZP	3	0	2.5	0
0.2 wt% Graphene-doped Y-TZP	2.994	0.006	2.495	0.005

3.1.2 Powder Mixing

Powder mixing between graphene and 3Y-TZP is a necessary step to produce a graphene-doped 3Y-TZP sample. Before the process of mixing, an adequate

amount of 3Y-TZP and graphene powders were prepared, as shown in Table 3.2 and Table 3.3. The mass of each powder was weighted precisely using electronic balance. Then, the graphene powders were subjected to supersonic bath in a beaker, followed by addition of 3Y-TZP powder into the same beaker. Stirring was required so that the powders did not stick to the bottom of beaker. After that, the mixtures were milled for about 1 hour. The next step was to dry the mixtures in a drying oven under 70 °C for 24 hours approximately. The dried mixture was then sieved into powders.

Table 3.2: Calculated Amount of 3Y-TZP and Graphene Powders Used for Mixing

Powder	Bar		Disc		Total	
	Number of Samples	Mass Required (g)	Number of Samples	Mass Required (g)	Number of Samples	Weight of Samples (g)
3Y-TZP	9	26.946	9	22.455	18	49.401
Graphene		0.054		0.045		0.099
Grand Total					<u>18</u>	<u>49.5</u>

Table 3.3: Actual Amount of 3Y-TZP and Graphene Powders Used for Mixing

Powder	Total Mass (g)	Actual Mass (g)
3Y-TZP	49.401	59.88
Graphene	0.099	0.12
Total	49.5	60

3.1.3 Green Body Preparation

After the mixture had been dried and sieved, it was pressed with the pressure about 70kgf/cm², using 5 Tonne Moulding Press. On the other hand, undoped 3Y-TZP was pressed without the need to perform powder mixing procedure. There were two types of die being used to prepare green body of samples, which

were rectangular and circular shape die. These dies will mould the samples into desired shapes accordingly. After that, both disc and bar samples were sent to IC-Innovation in Nanotechnology, SIRIM Berhad for cold isostatic pressing.

3.1.4 Sintering

Sintering is a process which apply heat below melting point to encourage bonding of particles. At the end of sintering process, the material is expected to have denser matrix with finer grain size. There are different sintering types such as hot isostatic pressing, spark plasma sintering, as well as pressureless sintering. In present work, pressureless sintering was conducted with the temperature at 1200 °C, 1300 °C and 1400 °C with 10 °C/min ramp rate. This temperature range was deemed to be appropriate for densification and mechanical properties improvement, according to one of the studies by Ramesh *et al.* (2016), with the holding time fixed at 2 hours.

In contrast with the research by Ramesh *et al.* (2016), this research revolved around three different parameters of sintering holding time, which were 6 minutes, 1 hour, and 2 hours respectively. Carbolite furnace of Constance, Germany was used for sintering of samples.

3.1.5 Grinding and Polishing (Disc Samples)

This step ensures the disc samples to have better surface finish for the sake of testing and analysis. Samples with good surface finish will improve the accuracy of the results obtained, especially in Vickers hardness test and scanning electron microscope (SEM). Firstly, the grinding of samples was done using silicon carbide sandpapers of distinct grade (180, 400, 600, 1000, 1500). Then, the surface of the samples was polished by using diamond compound (1µm and 5µm).

3.1.6 Thermal Etching (Disc Samples)

After grinding and polishing process, the disc samples were thermal etched in carbolite furnace (Constance, Germany) for 30 minutes. The thermal etching temperature was 50 °C lesser than the sintering temperature of that particular sample. For instance, if the sintering temperature was 1400 °C, then the thermal etching temperature would be 1350 °C.

3.1.7 Hydrothermal Ageing (Bar Samples)

The bar samples were firstly taken to XRD analysis in order to identify the monoclinic contents before aging period. After that, the samples were inserted into autoclave. The autoclave was then filled with distilled water until it could cover all the surface of samples. Then, the autoclave was heated up inside an oven under 180 °C for 12 hours. This allowed the hydrothermal aging to occur on the samples. Finally, the samples were taken out and dried, followed by XRD analysis for the second time to determine the changes in monoclinic contents of the samples.

3.2 Measurement of Results

After preparation of 3Y-TZP samples, they were tested in different aspects by utilising various equipment. As an overall view, bar samples were subjected to XRD analysis while disc samples were subjected to SEM analysis and mechanical properties analysis. At the end of measurement, the data obtained were analysed and discussed to make a logical conclusion. Sections below discuss the theoretical calculation of the data.

3.2.1 Measurement of Densification

The bulk density of both doped and undoped 3Y-TZP was identified via method of immersing the samples in water. A densification measurement kit was attached to an electronic balance for the quantification of density of samples. The relative density of each sample was calculated based on equation 3.1 and equation 3.2:

$$\rho = \frac{w_a}{w_a - w_w} \rho_w \quad (3.1)$$

Where,

ρ = bulk density of samples

w_a = weight of sample in air

w_w = weight of sample in water

ρ_w = weight of distilled water

$$\rho_r = \frac{\rho}{6.09} \times 100 \quad (3.2)$$

Where,

ρ_r = relative density

The value of 6.09g/cm³ indicates the theoretical density of 3Y-TZP.

3.2.2 Measurement of Vickers Hardness

Measurement of hardness of polished samples was carried out using Vickers Hardness Test, Eseway model. An indentation was performed to every sample by applying a load of 2kgf or up to 4kgf from pyramidal diamond indenter. After detaching the load, two impression diagonals were observed from the surface, known as D₁ and D₂. These values were measured by utilising Vickers Hardness equipment with a filar micrometer scaled to the nearest 0.1µm. By taking an average value of both D₁ and D₂, Vickers hardness was computed through equation 3.3:

$$H_v = \frac{1.854P}{D^2} \quad (3.3)$$

Where,

H_v = Vickers hardness

P = applied load

D = average value of D₁ and D₂

3.2.3 Measurement of Fracture Toughness

Aside from impression diagonals, the indentation from Vickers hardness test also produced four crack lines known as L₁, L₂, L₃ and L₄. These values were used to calculate mean crack length, L_{mean}. There are three methods that can be used to calculate fracture toughness, namely, Niihara, SWMC and Kaliszewski. The equation used in present work was from SWMC. The fracture toughness, K_{IC}, was then obtained by using equation 3.4:

$$K_{IC} = 0.0899 \times \left(\frac{H_v P}{4L_{mean}} \right)^{0.5} \quad (3.4)$$

Where,

H_v = Vickers hardness

P = applied load

L_{mean} = mean length

3.2.4 Measurement of Monoclinic Content

Monoclinic content could be used to indicate the aging resistance of samples, since hydrothermal aging is spontaneous phase transformation of (T) to (M) under lower temperature (Ramesh, Lee and Tan, 2018). Hence, the higher the amount of monoclinic content, the lower the aging resistance of samples. X-Ray diffraction (XRD) is a type of equipment that can be used to analyse the phase of 3Y-TZP samples. In current research, the XRD equipment used was Shimadzu Lab X, XRD-6000 from Japan.

The scan speed for the XRD analysis is 2 min/step (or 0.5 °/min), with the scan range of 27 ° to 36 ° (2 θ). The reason for choosing the following scan range is that the peak of tetragonal (t) can be found at ~30.37 °, while the two peaks of monoclinic (m) can be found at both ~28.2 ° and ~31.4 ° respectively. Every sample went through an equal amount of scan time of 5 min. As for the calculation, there were two equations involved:

$$X_m = \frac{(I_{(11\bar{1})m} + I_{(111)m})}{(I_{(111)c,t} + I_{(11\bar{1})m} + I_{(111)m})} \quad (3.5)$$

Where,

X_m = integrated intensity ratio

$I_{(111)m}$ = peak intensity at (111) plane, monoclinic

$I_{(111)c,t}$ = peak intensity at (111) plane, tetragonal

$I_{(11\bar{1})m}$ = peak intensity at (11 $\bar{1}$) plane, monoclinic

$$V_m = \frac{1.311 \times X_m}{(1 + 0.311 \times X_m)} \quad (3.6)$$

Where,

V_m = volume fraction of monoclinic

X_m = integrated intensity ratio, calculated from equation 3.5

Volume fraction can be expressed in percentage value through equation 3.7 below:

$$V_m \% = V_m \times 100\% \quad (3.7)$$

3.3 Research Flow Chart

The work plan of the research is summarised Figure 3.1.

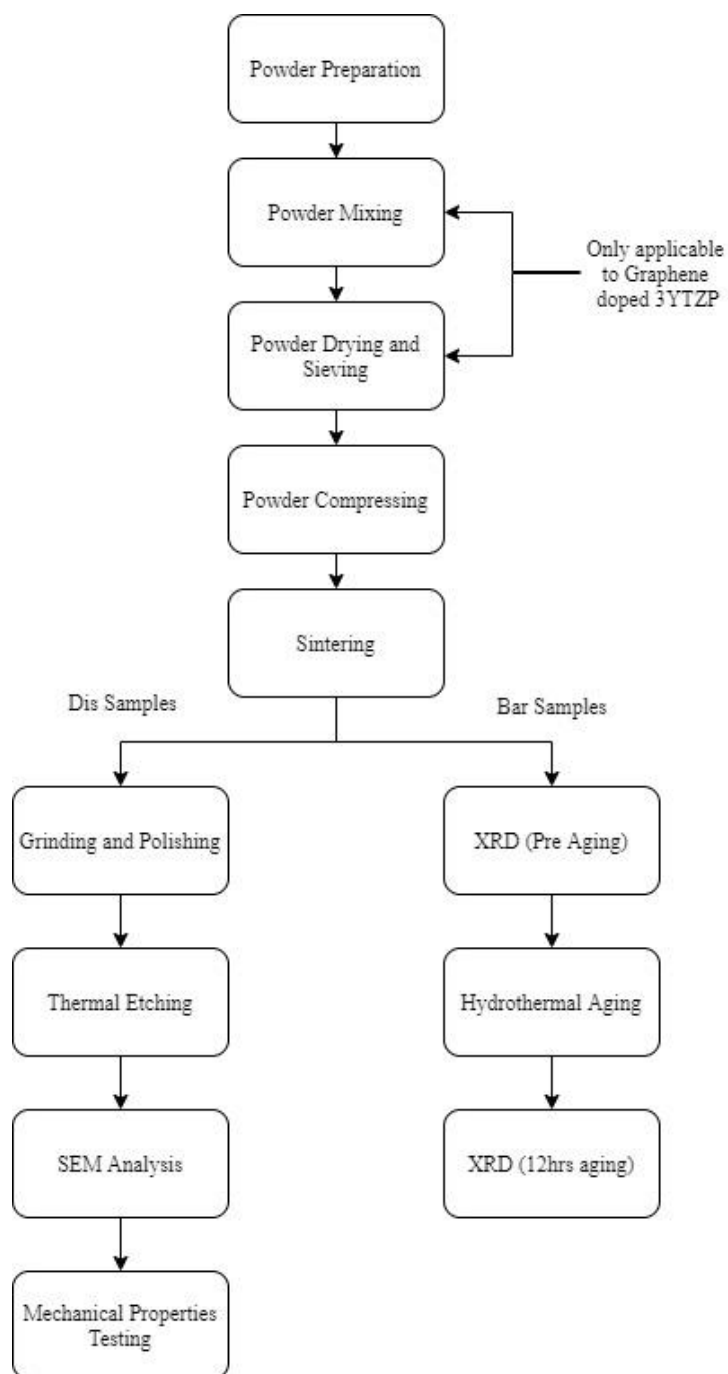


Figure 3.1: Research Methodology Flow Chart

CHAPTER 4

RESULTS AND DISCUSSION

4.1 XRD Phase Analysis (Pre-Aging)

The main purpose of XRD in this research is to identify the amount of monoclinic phase content with respect to tetragonal phase. Having a large amount of monoclinic phase content only shows that the sample would have suffered from hydrothermal aging process compared to those with fully tetragonal phase. On this research, the XRD analysis conducted on both 0.2 wt% graphene-doped 3Y-TZP and undoped 3Y-TZP samples showed that all of the samples exhibited fully tetragonal phase after sintering. These results correlated with the XRD analysis conducted by Ramesh *et al.* (2016), which discovered that the Y-TZP powder contained about ~17 % of monoclinic phase content, while Y-TZP sample after sintering contained fully tetragonal phase.

From Figure 4.1, 4.2 and 4.3, it can be observed that both graphene and pure 3Y-TZP has similar XRD pattern, in which all of the samples has peak intensity at $\sim 30.37^\circ$. This indicated that addition of 0.2 wt% of graphene dopant did not affect the stability of tetragonal phase of 3Y-TZP.

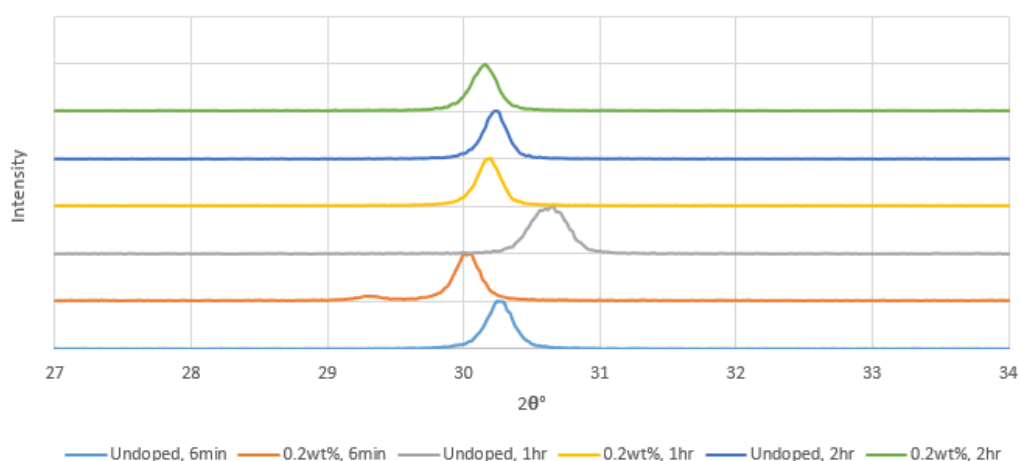


Figure 4.1: XRD Plot of Graphene Doped and Undoped 3Y-TZP at 1200 °C Sintering Temperature

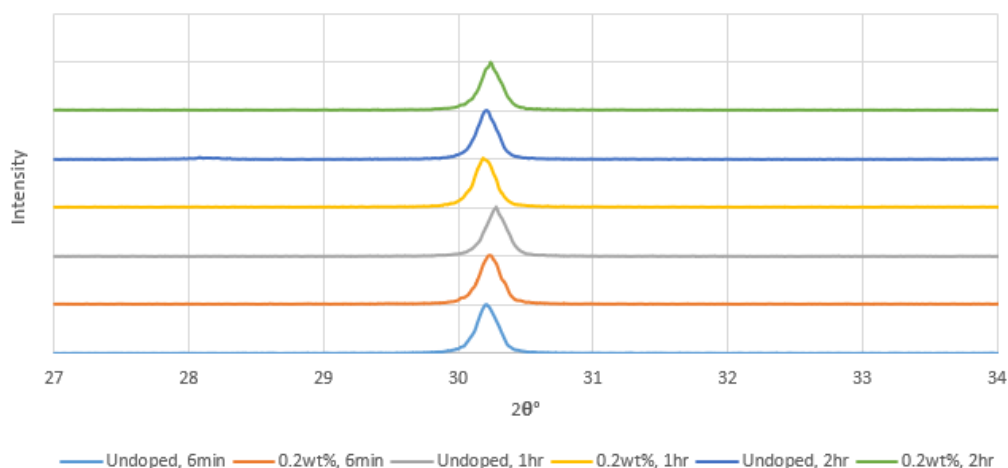


Figure 4.2: XRD Plot of Graphene Doped and Undoped 3Y-TZP at 1300 °C Sintering Temperature

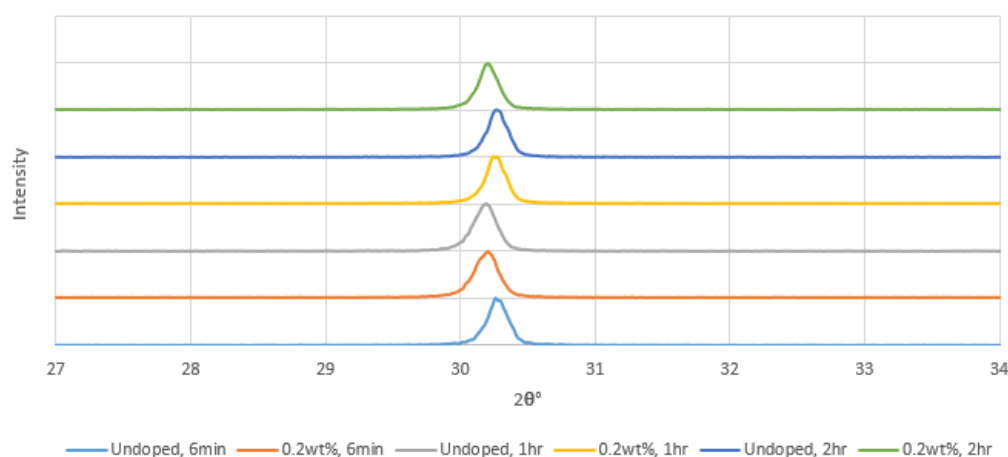


Figure 4.3: XRD Plot of Graphene Doped and Undoped 3Y-TZP at 1400 °C Sintering Temperature

4.2 XRD Phase Analysis (12 hrs Hydrothermal Aging)

Development of monoclinic content of 3Y-TZP samples after 12 hours of hydrothermal aging under 180 °C is shown in Table 4.1. Generally, a large amount of monoclinic content would disturb the stability of tetragonal structure, which in turn leads to further deterioration in mechanical properties (Ramesh, Lee and Tan, 2018) . A research by Ramesh and Gill (2001) unveiled that the increase in monoclinic content was proportional to the ageing duration until it reached a saturation level. In their study, undoped Y-TZP samples under sintering conditions of 1300 °C / 2 hr experienced increase in monoclinic

content up to ~80 % at the aging period of 50 hr. The percentage remained unchanged after 50 hr until 200 hr.

Looking into present study, it is undeniable that the aging of 12 hours would provide little changes to the monoclinic content. At low sintering temperature of 1200 °C, it was observed that there was 0 % of monoclinic content on both graphene doped and undoped 3Y-TZP even after 12 hours of hydrothermal aging duration. The result was almost similar at the sintering temperature of 1300 °C, except for the undoped 3Y-TZP sample at 2 hr sintering holding time. For this particular sample, it was noticed that there was a 4.66 % increase in monoclinic content. At the same time, its graphene doped 3Y-TZP counterpart remained at 0 %.

Furthermore, at sintering temperature of 1400 °C, the monoclinic content after 12 hr aging for undoped 3Y-TZP had risen to 4.45 % and 4.71 % at sintering time of 1 hr and 2 hr respectively. Both of the percentages were slightly higher than the graphene doped 3Y-TZP. In fact, almost all of the graphene doped 3Y-TZP remained undisturbed by 12 hr of hydrothermal aging. In a nutshell, addition of 0.2 wt% of graphene was proven to provide better hydrothermal aging resistance (up to 12 hr) to 3Y-TZP through this research.

Another point which should be taken into account from Table 4.1 is that all 3Y-TZP samples had excellent hydrothermal aging resistance up to 12 hr at short sintering holding time of 6 min. This result remained similar at the sintering temperature range between 1200 °C to 1400 °C.

Table 4.1: Monoclinic Content Percentage (%) of 3Y-TZP Samples at Different Sintering Conditions Under Hydrothermal Aging at 180 °C

Sintering Temperature/ Sintering Time	Ageing Time	Monoclinic Content of 0.2 wt% Graphene-doped 3Y-TZP	Monoclinic Content of Undoped 3Y-TZP
1200 °C / 6 min	0 hr	0	0
	12 hr	0	0
1200 °C / 1 hr	0 hr	0	0
	12 hr	0	0
1200 °C / 2 hr	0 hr	0	0
	12 hr	0	0
1300 °C / 6 min	0 hr	0	0
	12 hr	0	0
1300 °C / 1 hr	0 hr	0	0
	12 hr	0	0
1300 °C / 2 hr	0 hr	0	0
	12 hr	0	4.66
1400 °C / 6 min	0 hr	0	0
	12 hr	0	0
1400 °C / 1 hr	0 hr	0	0
	12 hr	3.92	4.45
1400 °C / 2 hr	0 hr	0	0
	12 hr	0	4.71

4.3 Mechanical Properties Analysis

4.3.1 Relative Density

The relative density of graphene doped and undoped 3Y-TZP at different sintering temperature and time is shown in Figure 4.4 below.

As an overall view, the relative density of undoped 3Y-TZP samples were at an increasing trend from 1200 °C to 1300 °C sintering temperature. Above 1300 °C, the relative density of undoped 3Y-TZP did not show any significant improvement. The undoped 3Y-TZP samples had the highest relative density at sintering conditions of 1400 °C, 1 hr, with the percentage of 98.49 %. In contrast, it had the lowest relative density at sintering conditions of 1200 °C, 6 min, with the percentage of 70.74 %. This showed that at higher sintering temperature, the relative density of the samples was generally higher.

On the other hand, the relative density of graphene doped 3Y-TZP showed similar trend as undoped 3Y-TZP. It had the highest relative density of 97.83 % at condition of 1400 °C, 2 hr, and had the lowest relative density of 72.09 % at condition of 1200 °C, 6 min.

As for the sintering holding time, both doped and undoped samples had higher relative density at 1 hr and 2 hr holding time, compared to 6 min holding time. However, the difference was much apparent at lower sintering temperature of 1200 °C. The only exception to such trend was found at 1400 °C sintering temperature of graphene doped 3Y-TZP, in which the sample at 6 min holding time had slightly higher relative density (97.54 %) compared to sample at 1 hr holding time (96.50 %).

By comparing both doped and undoped 3Y-TZP, it was determined that at lower sintering temperature of 1200 °C, addition of 0.2 wt% graphene to 3Y-TZP could yield better results of relative density compared to pure 3Y-TZP. The results were similar at 1300 °C, but the increase was less noticeable. On the contrary, at 1400 °C, undoped 3Y-TZP yielded better relative density compared to graphene doped 3Y-TZP. As such, addition of graphene dopant to 3Y-TZP at higher sintering temperature was found to be less beneficial for the relative density.

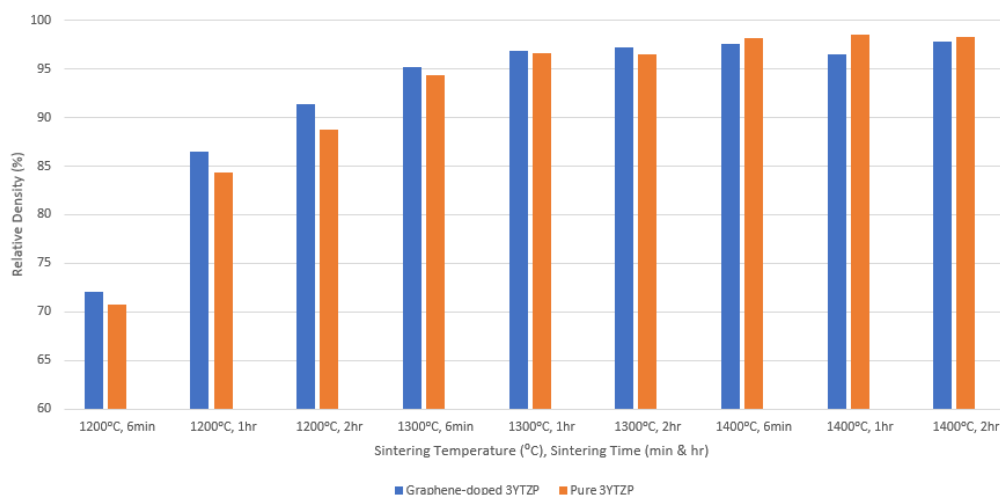


Figure 4.4: Relative Density against Sintering Temperature and Sintering Time for 3Y-TZP

4.3.2 Vickers Hardness

Figure 4.5 shows the graph of Vickers hardness of doped and undoped 3Y-TZP at different sintering conditions. Some authors proved that undoped Y-TZP samples achieved the maximum Vickers hardness at 14.1 GPa at sintering condition of 1300 °C, 2 hr (Ramesh *et al.*, 2016). Result in present work showed resemblance to previous research, in which undoped 3Y-TZP sample attained highest Vickers hardness (14.58 GPa) at similar sintering condition.

At low sintering temperature of 1200 °C, 0.2 wt% graphene doped 3Y-TZP samples were found to be higher than undoped 3Y-TZP in terms of Vickers hardness. Similar trend was observed at high sintering temperature of 1400 °C. In fact, the sintering condition which produces maximum Vickers hardness of 14.81 GPa was found at graphene doped 3Y-TZP, at 1400 °C, 6 min. The only case in which undoped 3Y-TZP samples were found to have higher Vickers hardness was at sintering conditions of 1300 °C, 1 hr and 1300 °C, 2 hr respectively. Generally, addition of 0.2 wt% graphene to 3Y-TZP at 1200 °C and 1400 °C did help to improve the Vickers hardness.

Another trend which was observed was that at sintering temperature of 1200 °C and 1300 °C, longer sintering holding time was observed to produce much higher Vickers hardness in both doped and undoped 3Y-TZP samples, with the only exception at holding time of 1 hr at 1200 °C. Even so, at 1400 °C sintering temperature, prolonged sintering holding time produced opposite

effect to the Vickers hardness of both type of samples, with the decreasing trend observed.

Both crystal structure and porosity are factors which contribute to the hardness of a material. Considering that the graphene doped sample at 1400 °C, 6 min sintering conditions had achieved fully tetragonal phase as well as considerably high relative density compared to other samples, it is undoubtedly that this sample appeared to have highest Vickers hardness value.

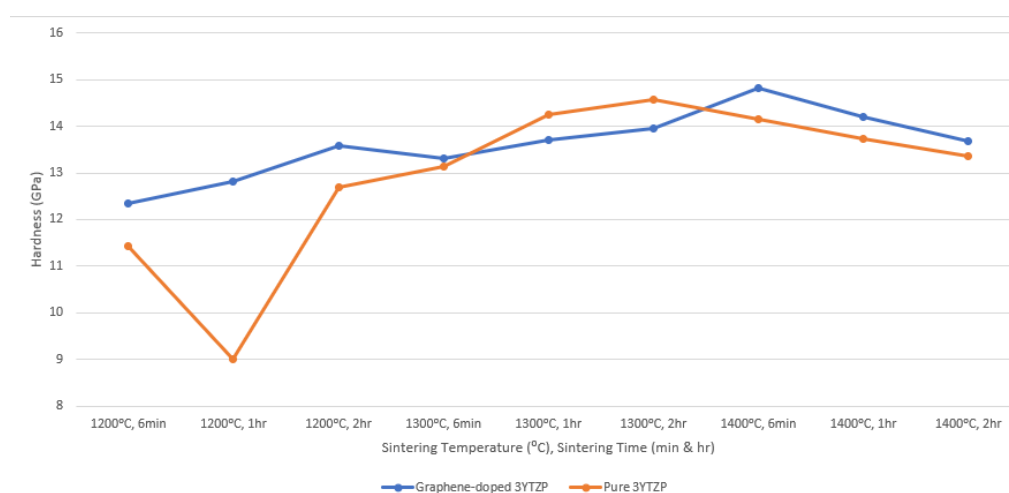


Figure 4.5: Vickers Hardness against Sintering Temperature and Sintering Time for 3Y-TZP

4.3.3 Fracture Toughness

Fracture toughness results of both doped and undoped 3Y-TZP samples are summarised in Figure 4.6. From the study of Turon-Vinas and Anglada, (2018) fracture toughness was said to be related to transformation toughening. Other factors that may manipulate the fracture toughness were grain size and sintering condition. Commonly, the fracture toughness value ranged from 4 MPa m^{1/2} to 8 MPa m^{1/2} for a pure Y-TZP. Another research revealed that the fracture toughness of Y-TZP was around 8 MPa m^{1/2} to 10 MPa m^{1/2} (Sivaraman *et al.*, 2018). The difference of values from both studies may be resulted from the origination of the Y-TZP powder. In this research, the 3Y-TZP powder used was originated from TOSOH, Japan.

At first glance, the fluctuating trend was observed in the undoped 3Y-TZP samples, with the highest peak of 9.01 MPa m^{1/2} at sintering condition of

1300 °C, 6 min. From the trend, it also showed that the fracture toughness of undoped 3Y-TZP samples were typically higher at 1300 °C sintering temperature, far exceeding graphene doped 3Y-TZP counterparts.

Addition of 0.2 wt% of graphene to 3Y-TZP resulted in a more stable trend of fracture toughness. The maximum fracture toughness for graphene doped 3Y-TZP was observed at sintering condition of 1400 °C, 6 min, with the value of 6.83 MPa m^{1/2}, higher than undoped 3Y-TZP at similar sintering condition. In addition, another trend was shown in which lower sintering holding time at 6 min produces graphene doped 3Y-TZP with higher fracture toughness compared to long holding time, irrespective of the sintering temperature. Nevertheless, addition of 0.2 wt% graphene was only effective in improving fracture toughness of 3Y-TZP at high sintering temperature of 1400 °C, with slight difference in values.

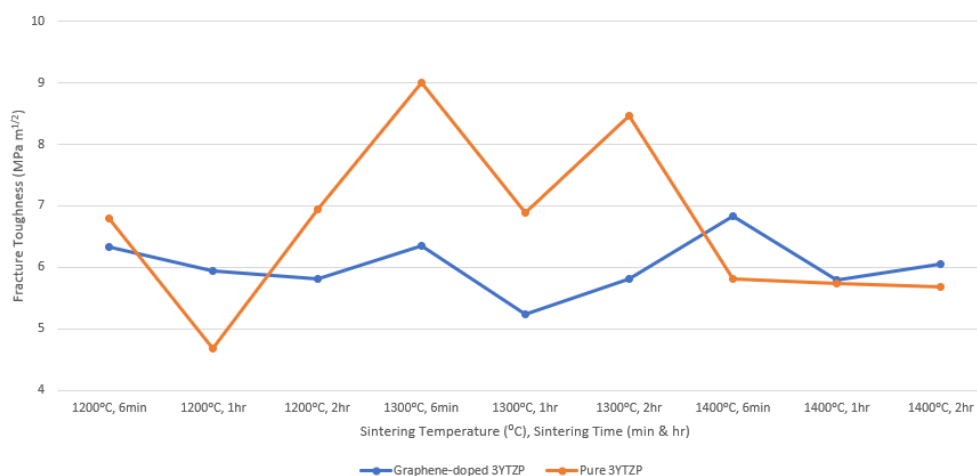


Figure 4.6: Fracture Toughness against Sintering Temperature and Sintering Time for 3Y-TZP

4.4 SEM Analysis

Scanning Electron Microscope (SEM) analysis is conducted in this research with a sole purpose to study the microstructure development and grain size of 3Y-TZP samples. By looking into differences in microstructure and grain size, a better comparison could be drawn between graphene doped and undoped 3Y-TZP. On top of that, the effect of sintering condition on microstructure development and grain size could also be studied.

Figure 4.7 shows microstructure images of selected 3Y-TZP samples obtained from SEM analysis. In Figure 4.7, (a), (b) and (c) represents undoped 3Y-TZP samples at 6 min, 1 hr and 2 hr sintering holding time respectively. Similarly, (d), (e) and (f) represents 0.2 wt% graphene doped, in ascending order of sintering time. Prior to SEM analysis, all the samples had been polished and thermal etched.

In general, there was no observable difference in the average grain size and grain morphology at different sintering holding time. By comparing the average grain size to the $2.00\mu\text{m}$ scale in figure, it was revealed that both doped and undoped 3Y-TZP had average grain size ranging from $\sim 0.2\mu\text{m}$ to $\sim 0.3\mu\text{m}$. Typically, the average grain size of doped and undoped 3Y-TZP at sintering temperature of $1200\text{ }^\circ\text{C}$ did not exceed $0.3\mu\text{m}$, regardless of the type and amount of dopants, as proven by both Ramesh *et al.* (2016) which used GO and Ramesh *et al.* (2011) which used MnO. Hence, addition of graphene additive did not produce changes on the grain morphology and average grain size of 3Y-TZP at sintering temperature of $1200\text{ }^\circ\text{C}$.

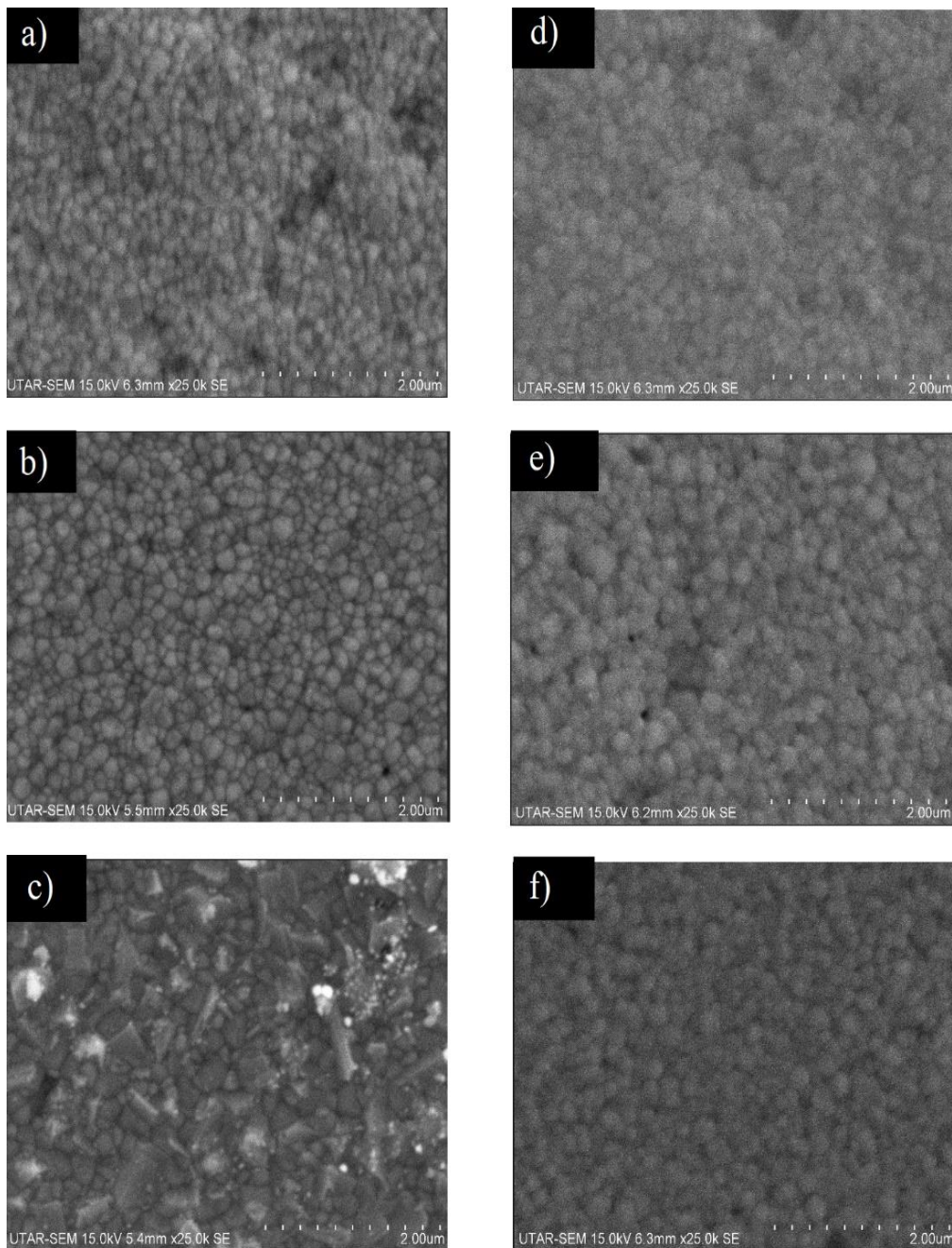


Figure 4.7: Microstructure Development for 3Y-TZP Samples at Sintering Temperature of 1200 °C [(a) Undoped 6 min, (b) Undoped 1 hr, (c) Undoped 2 hr, (d) 0.2 wt% Graphene Doped 6 min, (e) 0.2 wt% Graphene Doped 1 hr, (f) 0.2 wt% Graphene Doped 2 hr]

CHAPTER 5

CONCLUSIONS AND RECOMMENDATIONS

5.1 Conclusions

For this research, the effect of 0.2 wt% graphene additive on 3Y-TZP under various sintering conditions were examined. Firstly, addition of 0.2 wt% of graphene dopant did not affect the stability of tetragonal phase of 3Y-TZP. It was proven that all samples exhibit fully tetragonal phase after sintering process of various temperature. Besides, sintering holding time also did not affect the tetragonal phase of 3Y-TZP.

Secondly, addition of 0.2 wt% of graphene was discovered to provide lower monoclinic content percentage to 3Y-TZP through this research. In addition, both doped and undoped 3Y-TZP samples were found to have 0 % monoclinic content percentage at sintering holding time of 6 min.

Thirdly, this study of 3Y-TZP mechanical properties involved relative density, Vickers Hardness and fracture toughness. At sintering temperature of 1200 °C, addition of 0.2 wt% graphene was found to be effective in improving the relative density of 3Y-TZP. However, all 3Y-TZP samples had higher relative density at sintering conditions of 1300 °C to 1400 °C, irrespective of sintering holding time.

Furthermore, graphene doped 3Y-TZP at 1200 °C and 1400 °C showed higher value of Vickers hardness compared to undoped 3Y-TZP. The highest recorded value was 14.81 GPa, which was found at graphene doped 3Y-TZP at sintering condition of 1400 °C, 6 min. On top of that, the data of fracture toughness showed fluctuation on both type of samples. The undoped samples fluctuated at the range of $\sim 4.5 \text{ MPa m}^{1/2}$ to $\sim 9 \text{ MPa m}^{1/2}$, while the graphene doped samples fluctuated at the range of $\sim 5 \text{ MPa m}^{1/2}$ to $\sim 7 \text{ MPa m}^{1/2}$. Nonetheless, addition of 0.2 wt% graphene resulted in slight increase in fracture toughness of 3Y-TZP at sintering temperature of 1400 °C.

The maximum fracture toughness for graphene doped 3Y-TZP was observed at sintering condition of 1400 °C, 6 min, with the value of $6.83 \text{ MPa m}^{1/2}$. This critical finding revealed that graphene doped 3Y-TZP at 1400 °C, 6

min sintering conditions showed promising result in terms of mechanical properties and resistance to hydrothermal aging. SEM microstructure images revealed that addition of 0.2 wt% graphene showed no impact on the average grain size of 3Y-TZP at temperature of 1200 °C.

5.2 Recommendations for Future Work

Even though the research had been conducted successfully, there are some rooms for improvements which could be taken into consideration for further in-depth studies. First and foremost, one of the essential experiments of sonic resonance could be carried out in future work to determine the value of Young Modulus for all samples. The data is not only useful in identifying and comparing the stiffness between 3Y-TZP samples, but also necessary in computing the fracture toughness of the samples via Niihara and Kaliszewski method. Hence, the effect of addition of graphene dopant and sintering condition on Young Modulus could be an interesting approach to discover more about the mechanical properties of 3Y-TZP.

Moreover, the hydrothermal aging for present work is only conducted at 12 hr period. It is highly recommended to extend the hydrothermal aging period up to 200 hours to study the percentage of changes in monoclinic contents. This approach would provide a bigger picture on how well a 3Y-TZP sample could cope with hydrothermal aging. It is important to note that the experiment of hydrothermal aging may require proper time management and planning, since it is a time-consuming process.

Addition of 0.2 wt% of graphene dopant on 3Y-TZP seems to show promising result in terms of structure stability and mechanical properties under sintering condition of 1400 °C, 6 min. Another study could be done by varying the weight percentage of graphene dopant under same sintering condition to determine the optimum amount of dopant required to achieve enhancement in mechanical properties. Besides that, an alternative viewpoint for the case is by using different sintering method such as hot isostatic pressing and spark plasma sintering, instead of the pressureless sintering method used in this research. It is appealing to compare the result of 3Y-TZP samples from different sintering method.

REFERENCES

- Abd El-Ghany, O. S. and Sherief, A. H., 2016. Zirconia based ceramics, some clinical and biological aspects: Review. *Future Dental Journal*, Elsevier Ltd, 2(2), pp. 55–64. doi: 10.1016/j.fdj.2016.10.002.
- Aragón-Duarte, M. C. *et al.*, 2017. Nanomechanical properties of zirconia-yttria and alumina zirconia- yttria biomedical ceramics, subjected to low temperature aging. *Ceramics International*, Elsevier, 43(5), pp. 3931–3939. doi: 10.1016/j.ceramint.2016.12.033.
- Boniecki, M. *et al.*, 2017. Alumina / zirconia composites toughened by the addition of graphene flakes. 43(April), pp. 10066–10070. doi: 10.1016/j.ceramint.2017.05.025.
- Chen, F. *et al.*, 2015. Field assisted sintering of graphene reinforced zirconia ceramics. *Ceramics International*, Elsevier, pp. 1–4. doi: 10.1016/j.ceramint.2014.12.147.
- Chew Wai Jin, K., Minggat, M. M. A. M. and Singh, R., 2018. Sintered properties of stainless steel-doped Y-TZP ceramics. *MATEC Web of Conferences*, 152, p. 02012. doi: 10.1051/mateconf/201815202012.
- Hannink, R. H. J., Kelly, P. M. and Muddle, B. C., 2004. Transformation toughening in zirconia-containing ceramics. *Journal of the American Ceramic Society*, 83(3), pp. 461–487. doi: 10.1111/j.1151-2916.2000.tb01221.x.
- Liu, J. *et al.*, 2017. Materials science & engineering a spark plasma sintering of graphene platelet reinforced zirconia composites with improved mechanical performance. *Materials Science & Engineering A*. Elsevier B.V., 688(December 2016), pp. 70–75. doi: 10.1016/j.msea.2017.01.107.
- Martin, J., 2006. *Materials for engineering, Third Edition*. doi: 10.1201/9781439833124.
- Naveau, A., Rignon-Bret, C. and Wulfman, C., 2019. Zirconia abutments in the anterior region: A systematic review of mechanical and esthetic outcomes. *Journal of Prosthetic Dentistry*, Editorial Council for the Journal of Prosthetic Dentistry, 121(5), pp. 775-781.e1. doi: 10.1016/j.prosdent.2018.08.005.
- Obradovi, N. and Kern, F., 2018. Properties of 3Y-TZP zirconia ceramics with graphene addition obtained by spark plasma sintering. 44(May), pp. 16931–16936. doi: 10.1016/j.ceramint.2018.06.133.
- Ramesh, S. *et al.*, 2011. Densification behaviour and properties of manganese oxide doped Y-TZP ceramics. 37, pp. 3583–3590. doi: 10.1016/j.ceramint.2011.06.014.
- Ramesh, S. *et al.*, 2016. Sintering behaviour and properties of graphene oxide-

doped Y-TZP ceramics. *Ceramics International*, Elsevier, 42(15), pp. 17620–17625. doi: 10.1016/j.ceramint.2016.08.077.

Ramesh, S. and Gill, C., 2001. Environmental degradation of CuO-doped Y-TZP ceramics. 27, pp. 705–711.

Ramesh, S., Lee, K. Y. and Tan, C. Y., 2018. A review on the hydrothermal ageing behaviour of Y-TZP ceramics. *Ceramics International*, Elsevier Ltd and Techna Group S.r.l., 44(17), pp. 20620–20634. doi: 10.1016/j.ceramint.2018.08.216.

Schünemann, F. H. *et al.*, 2019. Zirconia surface modifications for implant dentistry. *Materials Science and Engineering C*, Elsevier B.V., 98, pp. 1294–1305. doi: 10.1016/j.msec.2019.01.062.

Shabalin, I. L., 2015. Ceramics, glasses, Composite materials part 1. Introduction : Definition. 2(April). doi: 10.13140/RG.2.1.4181.4568.

Sivaraman, K. *et al.*, 2018. Is zirconia a viable alternative to titanium for oral implant? A critical review. *Journal of Prosthodontic Research*, Japan Prosthodontic Society, 62(2), pp. 121–133. doi: 10.1016/j.jpor.2017.07.003.

Swab, J. J., 1991. Low temperature degradation of Y-TZP materials. *Journal of Materials Science*, 26(24), pp. 6706–6714. doi: 10.1007/BF02402664.

Turon-Vinas, M. and Anglada, M., 2018. Strength and fracture toughness of zirconia dental ceramics. *Dental Materials*, The Academy of Dental Materials, 34(3), pp. 365–375. doi: 10.1016/j.dental.2017.12.007.

Woodford, C., 2019. *Ceramics*. Retrieved from <https://www.explainthatstuff.com/ceramics.html> [Accessed 5 July 2019].

Zhang, Y. and Lawn, B. R., 2019. Evaluating dental zirconia. *Dental Materials*, The Academy of Dental Materials, 35(1), pp. 15–23. doi: 10.1016/j.dental.2018.08.291.

APPENDICES

APPENDIX A: Experiment Apparatus

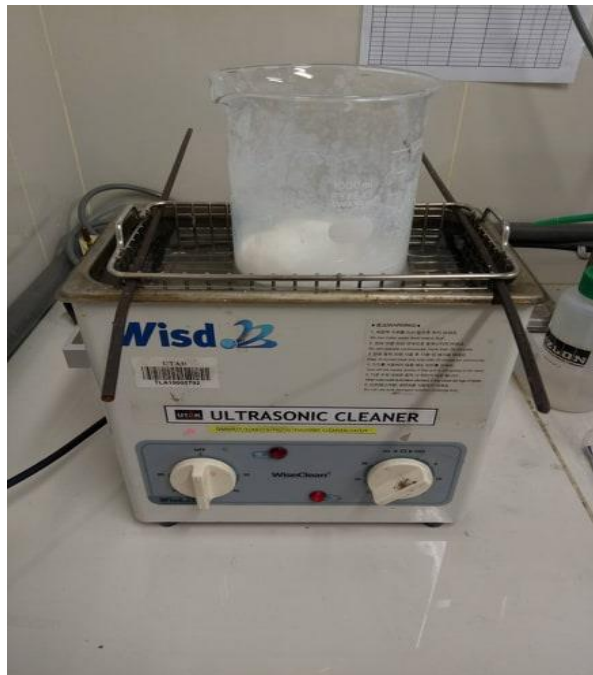


Figure A-1: Ultrasonic Cleaning of Powders Mixture (Graphene and 3Y-TZP)



Figure A-2: Ball Milling Process for 1 Hour to Evenly Distribute the Graphene in 3Y-TZP



Figure A-3: The Mixture of Powder is Dried in Drying Oven for 24 hours under 70 °C



Figure A-4: An Electronic Balance is Used to Measure the Precise Amount of Undoped 3Y-TZP Powder for Disc Sample



Figure A-5: Crushing and Sieving the Mixture Powder after Drying Process to Form Fine Powder



Figure A-6: 5 Tonne Moulding Press Used for Compacting the Powder in Green Body Preparation Process



Figure A-7: Preparation to Insert the Undoped 3Y-TZP into Die in Laboratory

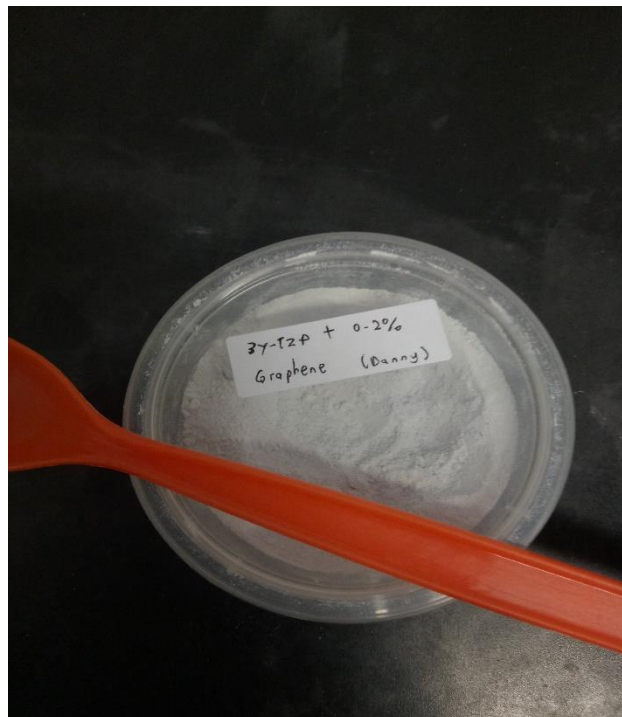


Figure A-8: 0.2 wt% Graphene Doped 3Y-TZP Powder Packed in Container

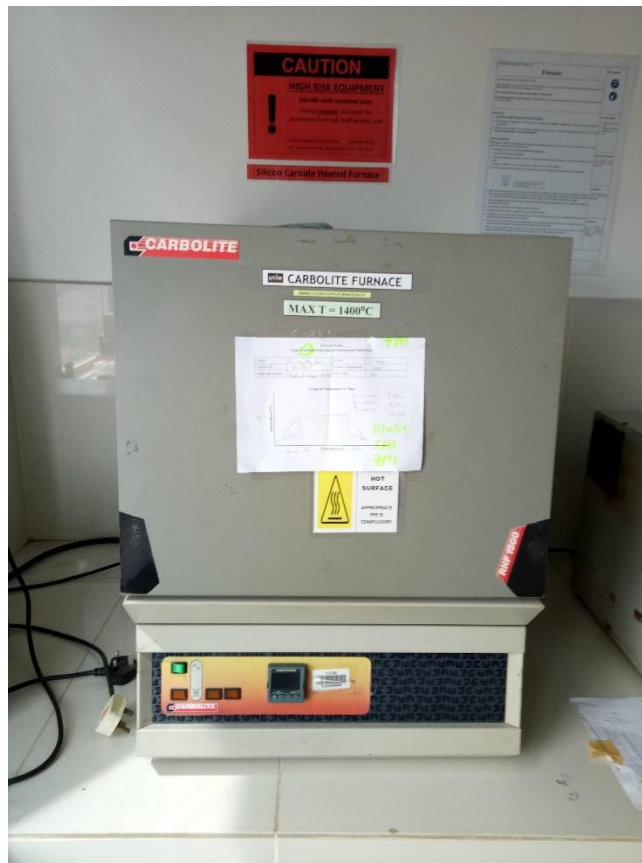


Figure A-9: Carbolite Furnace Used for Sintering and Thermal Etching of 3Y-TZP Samples

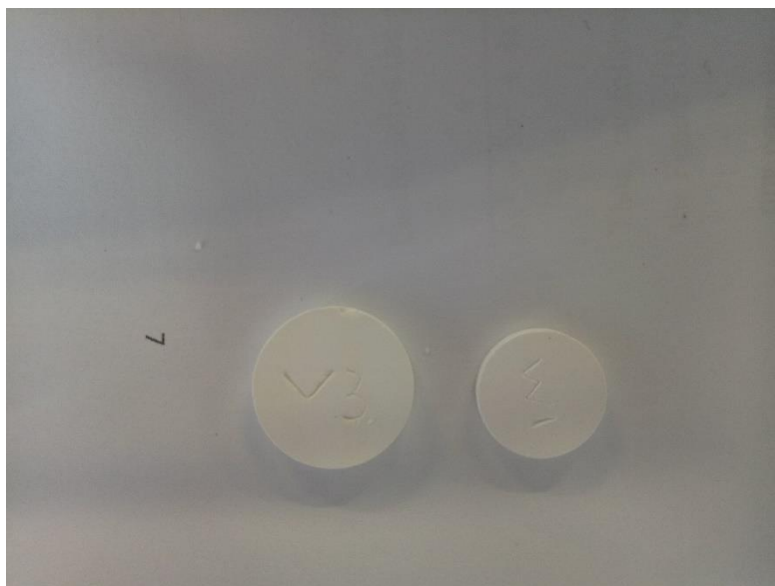


Figure A-10: Size of Undoped 3Y-TZP Samples Before (left) and After (right) Sintering

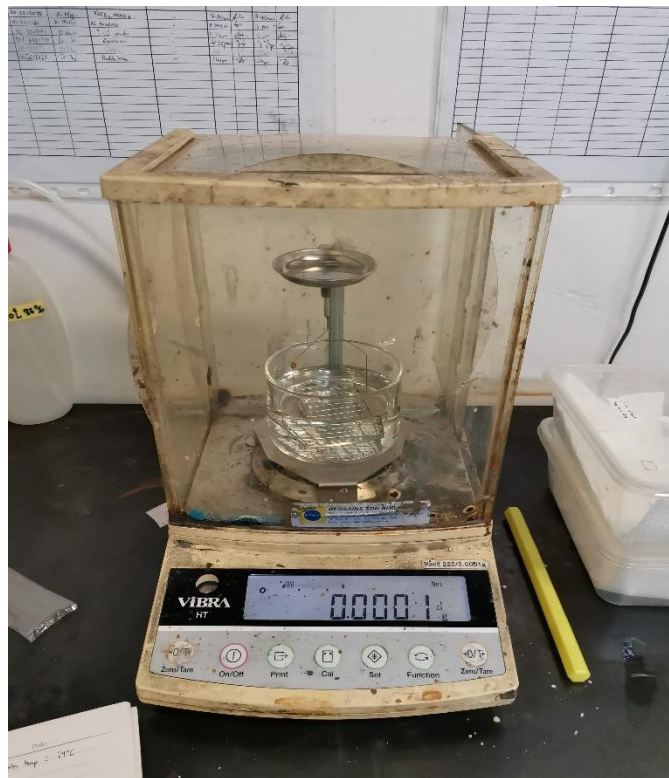


Figure A-11: Densification Measurement Kit Attached on Electronic Balance to Measure the Relative Density of 3Y-TZP Samples



Figure A-12: Grinding Machine Used for Grinding and Polishing of 3Y-TZP Samples

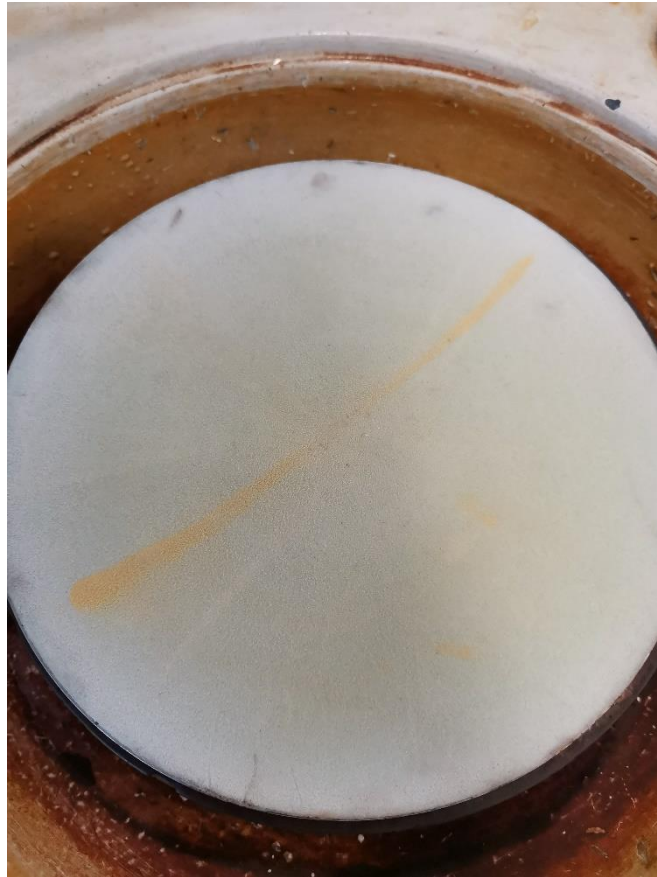


Figure A-13: Diamond Compound Applied for Polishing of Samples



Figure A-14: Vickers Hardness Tester Equipment Used for Vickers Hardness and Fracture Toughness Measurement

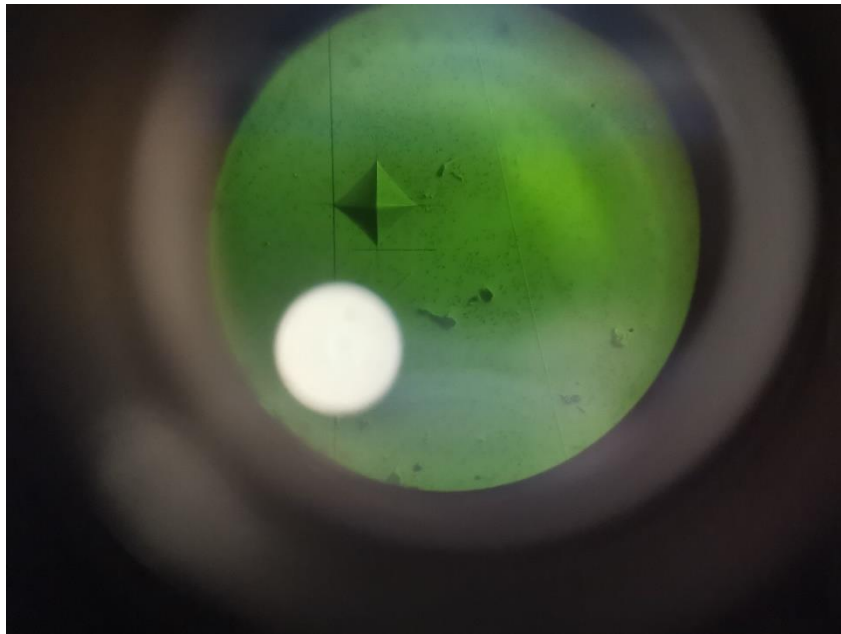


Figure A-15: Indentation on 3Y-TZP Sample by Vickers Hardness Tester



Figure A-16: Undoped 3Y-TZP Bar Sample Attached on Sample Holder for XRD Analysis



Figure A-17: Autoclave Used for Hydrothermal Aging of 3Y-TZP Samples



Figure A-18: Oven Used for Heating the Autoclave under 180 °C for 12 Hours

APPENDIX B: Density Chart of Water (g/cm^3) at Temperature of 0 °C to 39.9 °C

Reference:

Mass, Weight, Density or Specific Gravity of Water at Various Temperatures.

Available at: <https://www.simetric.co.uk/si_water.htm>

	0.0	0.1	0.2	0.3	0.4	0.5	0.6	0.7	0.8	0.9
0	0.999841	0.999847	0.999854	0.999860	0.999866	0.999872	0.999878	0.999884	0.999889	0.999895
1	0.999900	0.999905	0.999909	0.999914	0.999918	0.999923	0.999927	0.999930	0.999934	0.999938
2	0.999941	0.999944	0.999947	0.999950	0.999953	0.999955	0.999958	0.999960	0.999962	0.999964
3	0.999965	0.999967	0.999968	0.999969	0.999970	0.999971	0.999972	0.999972	0.999973	0.999973
4	0.999973	0.999973	0.999973	0.999972	0.999972	0.999972	0.999970	0.999969	0.999968	0.999966
5	0.999965	0.999963	0.999961	0.999959	0.999957	0.999955	0.999952	0.999950	0.999947	0.999944
6	0.999941	0.999938	0.999935	0.999931	0.999927	0.999924	0.999920	0.999916	0.999911	0.999907
7	0.999902	0.999898	0.999893	0.999888	0.999883	0.999877	0.999872	0.999866	0.999861	0.999855
8	0.999849	0.999843	0.999837	0.999830	0.999824	0.999817	0.999810	0.999803	0.999796	0.999789
9	0.999781	0.999774	0.999766	0.999758	0.999751	0.999742	0.999734	0.999726	0.999717	0.999709
10	0.999700	0.999691	0.999682	0.999673	0.999664	0.999654	0.999645	0.999635	0.999625	0.999615
11	0.999605	0.999595	0.999585	0.999574	0.999564	0.999553	0.999542	0.999531	0.999520	0.999509
12	0.999498	0.999486	0.999475	0.999463	0.999451	0.999439	0.999427	0.999415	0.999402	0.999390
13	0.999377	0.999364	0.999352	0.999339	0.999326	0.999312	0.999299	0.999285	0.999272	0.999258
14	0.999244	0.999230	0.999216	0.999202	0.999188	0.999173	0.999159	0.999144	0.999129	0.999114
15	0.999099	0.999084	0.999069	0.999054	0.999038	0.999023	0.999007	0.998991	0.998975	0.998959
16	0.998943	0.998926	0.998910	0.998893	0.998877	0.998860	0.998843	0.998826	0.998809	0.998792
17	0.998774	0.998757	0.998739	0.998722	0.998704	0.998686	0.998668	0.998650	0.998632	0.998613
18	0.998595	0.998576	0.998558	0.998539	0.998520	0.998501	0.998482	0.998463	0.998444	0.998424
19	0.998405	0.998385	0.998365	0.998345	0.998325	0.998305	0.998285	0.998265	0.998244	0.998224
20	0.998203	0.998183	0.998162	0.998141	0.998120	0.998099	0.998078	0.998056	0.998035	0.998013
21	0.997992	0.997970	0.997948	0.997926	0.997904	0.997882	0.997860	0.997837	0.997815	0.997792
22	0.997770	0.997747	0.997724	0.997701	0.997678	0.997655	0.997632	0.997608	0.997585	0.997561
23	0.997538	0.997514	0.997490	0.997466	0.997442	0.997418	0.997394	0.997369	0.997345	0.997320
24	0.997296	0.997271	0.997246	0.997221	0.997196	0.997171	0.997146	0.997120	0.997095	0.997069
25	0.997044	0.997018	0.996992	0.996967	0.996941	0.996914	0.996888	0.996862	0.996836	0.996809
26	0.996783	0.996756	0.996729	0.996703	0.996676	0.996649	0.996621	0.996594	0.996567	0.996540
27	0.996512	0.996485	0.996457	0.996429	0.996401	0.996373	0.996345	0.996317	0.996289	0.996261
28	0.996232	0.996204	0.996175	0.996147	0.996118	0.996089	0.996060	0.996031	0.996002	0.995973
29	0.995944	0.995914	0.995885	0.995855	0.995826	0.995796	0.995766	0.995736	0.995706	0.995676
30	0.995646	0.995616	0.995586	0.995555	0.995525	0.995494	0.995464	0.995433	0.995402	0.995371
	0.0	0.1	0.2	0.3	0.4	0.5	0.6	0.7	0.8	0.9